SANDIA REPORT

High-Temperature Split-Flow Recompression Brayton Cycle Initial Test Results

Steven A. Wright, Thomas M. Conboy, and Gary E. Rochau

Sandia National Laboratories

High-Temperature Split-Flow Recompression Brayton Cycle Initial Test Results

Steven A. Wright
Thomas M. Conboy
Gary A. Rochau

Advanced Nuclear Concepts
Sandia National Laboratories
P.O. Box 5800
Albuquerque, New Mexico 87185-1136

Abstract

Supercritical CO_2 (S-CO_2) power plants offer the potential for better economics because of their small size, use of standard materials, and improved electrical power conversion efficiency at modest temperature (400–750°C) [1]. Sandia National Laboratories (SNL or Sandia) and the U.S. Department of Energy Office of Nuclear Energy (DOE-NE) are operating a supercritical CO_2 Brayton cycle power system—the Generation IV (Gen IV) split-flow S-CO_2 compressor test loop—currently located in Arvada Colorado, at Barber Nichols, Inc., [2] under contract to Sandia. A photograph of the upgraded loop is shown in Figure E-1. This system is one of the first S-CO_2 power-producing Brayton cycles operating in the world. This report provides a summary of the newly installed hardware and briefly describes some of the test results that were performed in the upgraded split-flow Brayton loop during June and July of 2011.

The Gen IV S-CO_2 split-flow Brayton loop was reconfigured to operate as a simple heated recuperated Brayton loop for the testing in this report period. The test loop had just concluded a phase of construction that substantially increased the capability of the loop by adding heaters, a high-temperature (HT) recuperator, more waste heat removal capability, high-power load banks, larger diameter piping with more bends to reduce thermal stress, and more capable scavenging pumps to reduce windage and friction within the turbomachinery and provide greater cooling capabilities. With these additions, the loop greatly increased its capacity for electrical power generation (30–80 kWe per generator, depending on the loop configuration) and its ability to reach high temperatures (up to 810 K [1000°F]).

In recent weeks of testing, the test facility began to realize this potential by achieving new records in turbine inlet temperature (615 K [650°F]), shaft speed (52,000 rpm), pressure ratio (1.65), flow rate (2.7 kg/s), and electrical power generated (20 kWe). These operating conditions still remain short of design conditions for each turbine—an inlet temperature of 810 K (1000°F), a pressure ratio of 1.8, a shaft speed of 75,000 rpm, a flow rate of 3.5 kg/s, and a maximum generator power of 125 kWe—but they are beginning to be approached.

Not all planned upgrades were implemented due to the limited funding profile of FY2010. Only 520 kW of heater power were installed—not the total 780 kW. Furthermore, because one of the heater controllers was not functioning, only 390 kW of heater power were available. Similarly, the 3-in. piping was installed only in the high-pressure leg of the loop, not in the low-pressure leg, as was originally planned. We also had to rely on the new load bank capability for rapid shutdown situations, and were not able to install a dedicated shutdown resistor. Nevertheless, in spite of these limitations, we operated the loop at record operating conditions and were largely limited only by the facility and support equipment—not the turbomachinery.

The major observations from this round of testing are as follows:

1) The simple recuperated Brayton loops (with either the main compressor or the recompressor) behave very similarly to the previous configurations and produce about the same electric power for the same operating conditions.
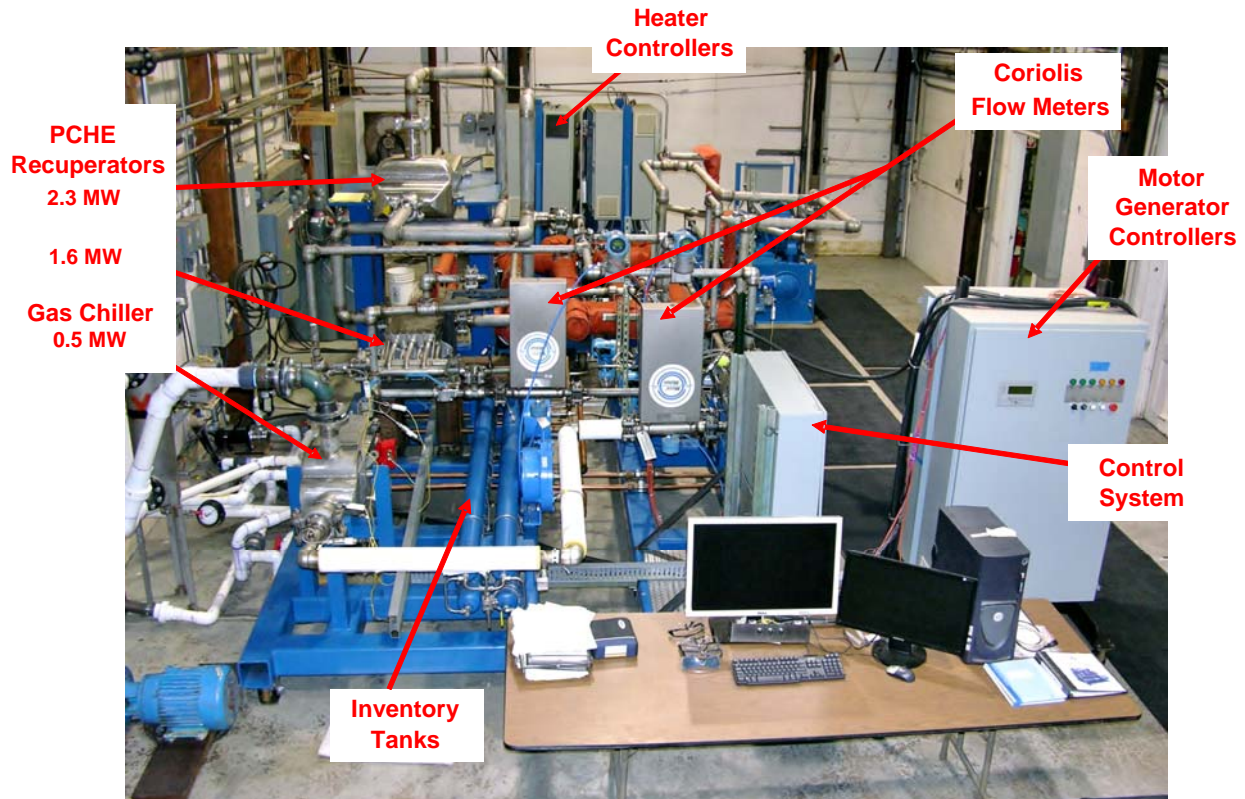
Figure E-1. Upgraded DOE Gen IV recompression loop.

The loop has 520 kW of installed heaters, two Printed Circuit Heat Exchanger (PCHE) recuperators, one PCHE gas chiller, two turbo-alternator-compressors (TACs), two motor generator controllers, a Hydro-Pac scavenging pump, and two 175-kW Avtron load banks (not shown), as well as a larger evaporative cooler (not shown).

2) The greater heater power and greater cooling capability allow the test loops to achieve greater operating temperatures and thus greater power generation while keeping the compressor inlet conditions just above the critical point.

3) The larger scavenging pump is very effective at reducing the rotor cavity pressure to approximately 1.4–2.0 MPa, which means that the gas-foil bearings run quite cool when the compressor is operated near the critical point.

4) The larger scavenging pump introduced flow oscillations in the early testing, but this was corrected in later tests by reinjecting the pumped fluid to the inlet of the gas chiller rather than the inlet of the main compressor.

5) The recompressor was operated at two inlet conditions. One set of experiments were performed with inlet conditions that were near the recompressor design conditions. Two other sets of experiments were performed at conditions that were very close to the main compressor design conditions (i.e., near the critical point). Because of its larger diameter, the recompressor was able to achieve near-design-flow conditions for the main compressor but at much lower shaft speeds. This means higher pressure ratios, greater flow at lower speeds, and much less friction and lower bearing temperatures. The startup process is also simpler for the recompressor. For these reasons, it is highly likely that we will modify the main

compressor to use the recompressor wheel rather than the main compressor wheel for many of the future split-flow tests.

6) Electrical power generation tests were performed at sufficiently high enough power levels that reasonable estimates of the major losses began to become apparent. Some of these losses can be reduced by making already-planned changes to the motor generator controller, while others may require modifications to the turbomachinery to reduce these losses. A brief summary of these losses are provided.

7) The primary limits observed to date are due to the cooling capability, which appears to be limited to approximately 280 kW. We are hopeful that as fall and winter approach, the cooling capability will improve as the atmospheric conditions cool.

The next phase of research (through December 2011) will focus on continuing to push the operating limits and proceeding with upgrades. Testing will shift from operating the simple recuperated Brayton loop to operating the split-flow S-CO$_2$ Brayton loop configuration based on using successful startup procedures developed in June of FY2010. It is expected that greater electrical power will be produced using the recompression loop because more heat can be recuperated.

Contents

Figures

Figures (cont.)

Tables

Nomenclature

DOE	U.S. Department of Energy
HT	high-temperature
IGBT	insulated gate bipolar transistor
LT	low-temperature
OSR	overspeed resistor
PCHE	printed circuit heat exchanger
s	seconds
S-CO$_2$	supercritical SO$_2$
TAC	turbo-alternator-compressor
TIT	turbine inlet temperature
UA	conductance-area product

INTRODUCTION

The U.S. Department of Energy (DOE) Advanced Reactors Program is developing a megawatt-class supercritical CO_2 (S-CO_2) Brayton-cycle test loop—the Generation IV (Gen IV) split-flow S-CO_2 compressor test loop—to investigate the key technical issues for this power cycle and to confirm model estimates of system performance. This report provides a summary of the progress achieved since January 2011 and includes descriptions of a number of upgrades and the test performance of the upgraded loop. The loop is currently located in Arvada, Colorado, at Barber Nichols, Inc., [2] under contract to Sandia.

The Gen IV split-flow S-CO_2 Brayton loop was reconfigured to operate as a simple heated recuperated Brayton loop for the testing in this report period. A schematic of the simple heated recuperated Brayton loop is shown in Figure 0-1. The image shows the loop as it existed in the summer of 2011 and includes recent facility upgrades. The test loop had just concluded a phase of construction that substantially increased the capability of the loop by adding heaters, a high-temperature (HT) recuperator, more waste heat removal capability, high-power load banks, larger diameter piping with more bends to reduce thermal stress, and more capable scavenging pumps to reduce windage and friction within the turbomachinery and provide greater cooling capabilities. With these additions, the loop greatly increased its capacity for electrical power generation (30–80 kWe per generator, depending on the loop configuration) and its ability to reach high temperatures (up to 810 K [1000°F]).

This report begins with a summary of the major hardware additions, then follows with a brief summary of recent experimental work that, in separate test configurations, showed break-even conditions in the main compressor turbomachinery and significant power production in the recompressor (20 kWe). These tests also resulted in other notable observations, including 1) superior performance of the Hydro-Pac scavenging pump, which resulted in reduced windage, lower bearing temperatures, and higher speeds achieved; 2) the importance of directing the Hydro-Pac plumbing outlet flow to a well-selected location of the loop; 3) successful operation of the load bank in dissipating generated electricity; and 4) the observation of a 'pinching' phenomenon within the high/low temperature printed circuit heat exchangers (PCHEs) as a result of the excessive recuperation capability installed at the current thermal power level.
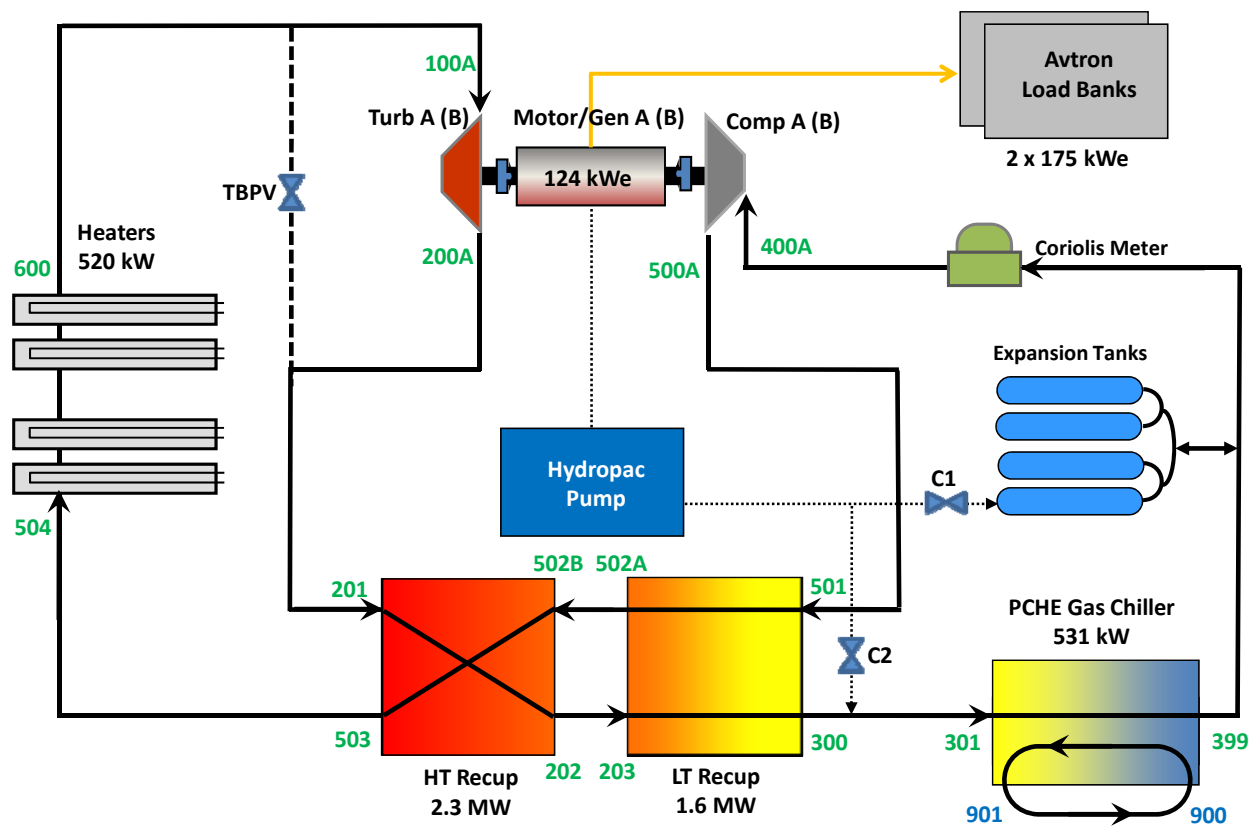
Figure 0-1: Flow schematic for the heated recuperated Gen-IV S-CO$_2$ Brayton loop.

This loop configuration is made from the split-flow power cycle by removing the recompressor turbomachinery and blocking off the ducting. Either the main turbomachinery (A) or the recompressor turbomachinery (B) can be used.

STATUS OF HARDWARE ADDITIONS AND UPGRADES

The DOE Gen IV split-flow $S-CO_2$ test loop completed a phase of construction and hardware upgrades in the summer of 2011 that increased the power generating capabilities of the test loop. The loop was modified to operate with two additional 130-kW heaters and an HT PCHE recuperator. An engineering schematic of the planned final design for this loop is shown in Figure 0-1. Much of the auxiliary equipment to run the system (not shown in the engineering drawing) was upgraded. This included an expanded gas cooling capability, new load banks, and a new gas scavenging pump. Substantial plumbing modifications were also made to accommodate the thermal stresses induced by the goal to reach full temperature and pressure (810 K [1000°F]). Each upgrade to the loop and the current status and plans for future upgrades are presented in the sections that follow.
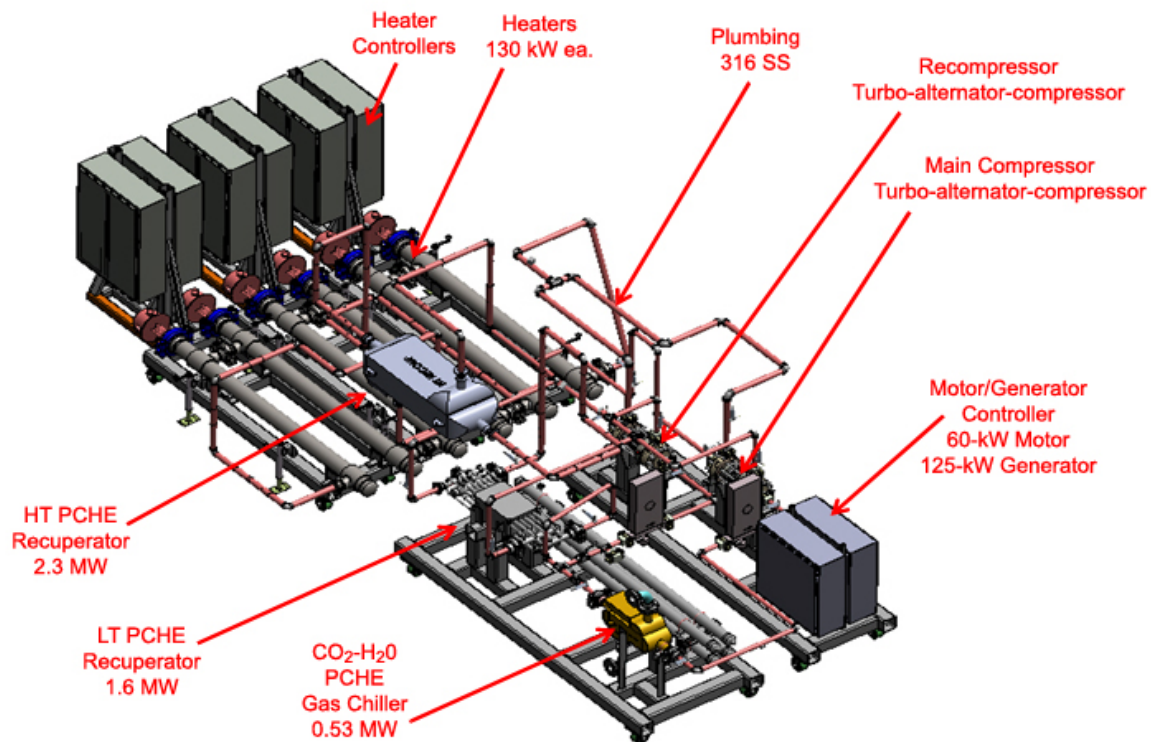
Figure 0-1. Engineering drawing of the piping layout for the $S-CO_2$ recompression Brayton Cycle.

Hardware Upgrade Status Summary

A large number of components were added to the Gen IV loop during the first period of FY2011. The components were installed to increase the turbine inlet temperature, better reject the waste heat, reduce windage/friction losses, and control the turbomachinery speed during power generation. These changes and upgrades were originally planned in FY2009, and contracts to implement them were placed as far back as 2009. The modifications and upgrades were needed to operate the turbomachinery at high temperatures and at high speeds to facilitate the production of electric power. Because one of the main objectives of this program is to generate electric power to evaluate the design tools and models, the upgrade effort has been one of the major

focuses of FY2011. Brief descriptions of the upgraded components are provided in Sections 2.2 through 2.5. A photograph of the upgraded loop as of May 2011 is shown in Figure 0-2.
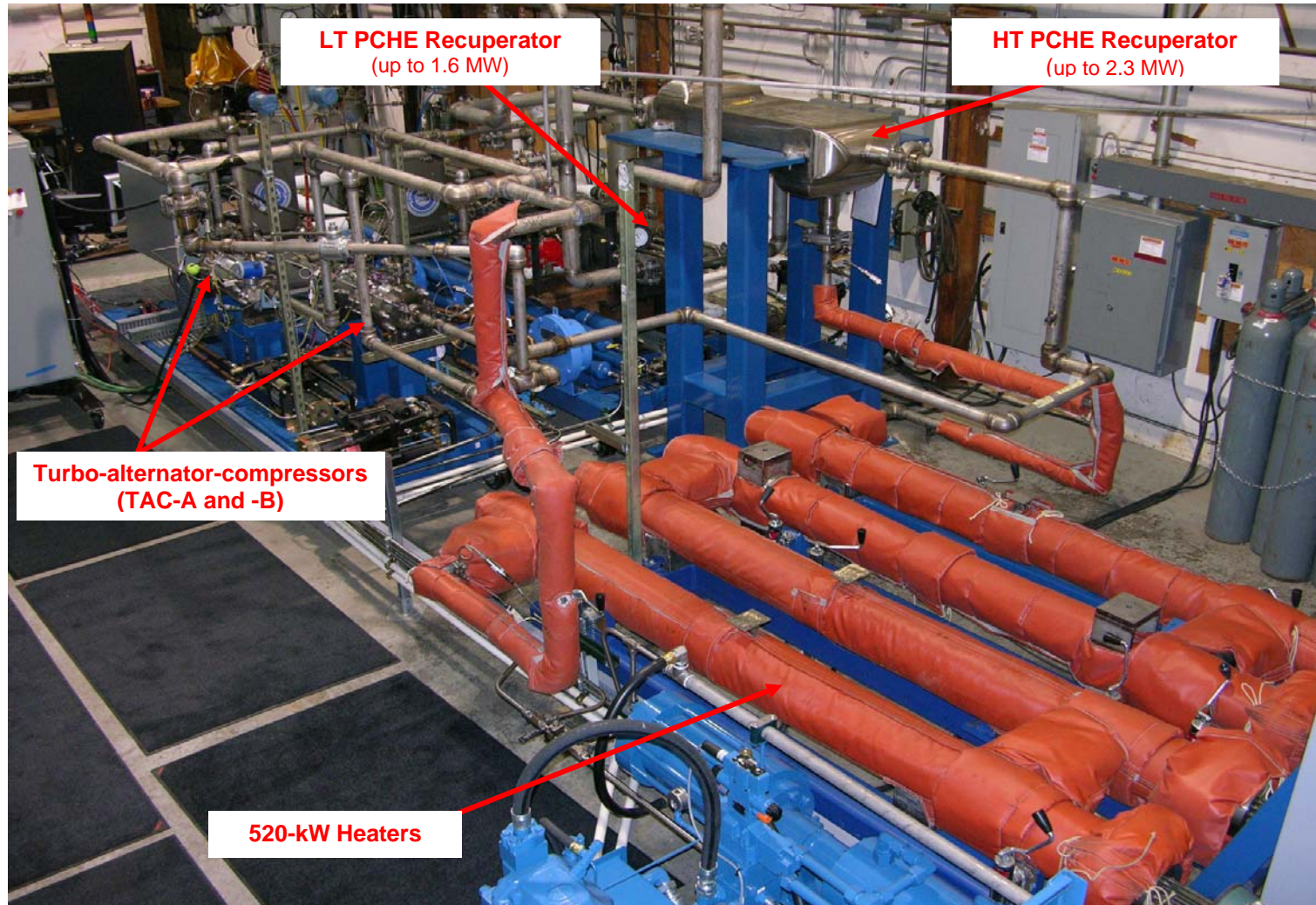
Figure 0-2. Fully assembled and instrumented Gen IV S-CO$_2$ split-flow heated recuperated Brayton cycle.

The photo was taken on May 26, 2011 and shows the installation with four of the six heaters installed.

High-Temperature (HT) and Low-Temperature (LT) PCHE Recuperators

An HT PCHE was purchased from Heatric in the United Kingdom [3] in November 2009 for use as the HT recuperator within the Gen IV split-flow Brayton loop. This component was the third PCHE heat exchanger to be installed in the loop. A photo of the HT recuperator is shown in Figure 0-3. The PCHE was delivered to Barber Nichols, Inc., in October 2010. It is constructed of 316 stainless steel and was designed to transfer 2.3 MW with a hot-side inlet temperature of 755 K (900°F). The recuperator and support frame were installed in the split-flow test loop following engineering analysis using the code Caesar II, to ensure suitable accommodation during thermal expansion. The approximate dimensions of the HT recuperator are provided in Table 0-1.

Figure 0-3. Gen IV S-CO$_2$ split-flow Brayton HT Recuperator.

Table 0-1. Approximate Dimensions of the HT PCHE Recuperator.

Property	Value
HT Recuperator	
Channel Width	1.27 mm (0.05 in.)
Channel Depth	0.77mm (0.0303 in.)
Plate Depth	1.69 mm (0.0665 in.)
Flow Area per Channel	0.768 mm^2 (0.00119 in.^{2})
Hydraulic Diameter (Dh)	1.0607 mm (0.0418 in.)
Core	
Height	0.296 m (11.65 in.)
Length	0.996 m (39.21 in.)
Width	0.512 m (20.16 in.)
Heat Transfer Area	43 m^2 (462.80 ft^2)
Core Mass	1410 kg (3108 lbm)

The low-temperature (LT) recuperator was installed in the loop in FY2010. A photo of the LT recuperator is provided in Figure 0-4, and the approximate heat transfer and flow dimensions of the recuperator are provided in Table 0-2. In general, the LT recuperator has smaller flow passages than the HT recuperator and approximately half the heat transfer area. It was also designed to function as the main recuperator in a simple recuperated Brayton cycle.

Figure 0-4. Gen IV S-CO$_2$ split-flow Brayton LT recuperator.

Table 0-2. Approximate Dimensions and Flow Area in the LT Recuperator.

Property	Value
LT Recuperator	
Channel Width	0.96 mm (0.0378 in.)
Channel Depth	0.66 mm (0.0260 in.)
Plate Depth	0.97 mm (0.0382 in.)
Flow Area per Channel	0.4976 mm^2 (0.000771 in.^{2})
Hydraulic Diameter (Dh)	0.8873 mm (0.0349 in.)
Core	
Height	0.3556 m (14 in.)
Length	0.5842 m (23 in.)
Width	0.254 m (10 in.)
Heat Transfer Area	18 m^2 (194 ft^2)
Core Mass	248.5 kg (548 lbm)

Two Additional 130-kW S-CO$_2$ Heaters

Two additional immersion heaters were purchased in FY2010, delivered to Barber Nichols late in FY2010, and installed in FY2011. These two heaters increase the total thermal power capability of the loop to 520 kW. With these additional heaters, there is sufficient power to reach high temperatures (>650 K), and the Brayton loop should be capable of making electrical power in all configurations, provided sufficient cooling is available. Some configurations should be able to reach the design temperature of 810 K (1000°F). At 520 kW, the heaters alone command far more electrical power than can be provided by the Barber Nichols test facility; therefore, during testing, diesel generators were rented to supply the needed electrical power. One of the smaller diesel generator sets that we used is shown in Figure 0-5. At the time of the testing described here, one of the Watlow® heater controllers malfunctioned. It was returned to the manufacturer for repair. This limited the heater power to 390 kW rather than the expected 520 kW.

To finalize the build of the S-CO$_2$ loop as designed, a fifth and sixth set of heaters must be ordered, manufactured, and installed into the loop. This will be done when sufficient funding is available. The present modifications have been made with the final assembly in mind, so that the last heater upgrade will be a relatively simple modification in terms of rearranging the loop plumbing. The last two heaters will give the loop its full operating capability of 0.78 MW and will allow all configurations to reach the turbine inlet design temperature of 810 K (1000°F).

There will be insufficient facility power and cooling at the Barber Nichols test site to operate the loop at its eventual capacity (0.78 MW). Therefore, the Sandia development plan has been to extend the limiting features of the loop and turbomachinery within the confines of a 0.52-MW heated S-CO$_2$ Brayton loop. During this period, it is expected that researchers will identify inefficiencies and losses that can be mitigated and other limits such as those that might be caused by loop pressure drop or rotor cavity windage.

Figure 0-5. The Avtron Load Banks (l) and a Diesel Generator Set Rental (r).

The resolution of these issues will likely require minor modifications to the loop or turbomachinery. Once these modifications are made, the loop will be shipped to Sandia. The Sandia test site has sufficient capability to run the loop at its full power and cooling conditions. Some modifications to the SNL facility may be required, such as improvements to the cooling pumps, rerouting of electrical disconnects to interface more easily with the Brayton loop, installation of the new load banks, and potential gas chiller upgrades. The major tasks in FY2012 may be the disassembly, shipping, reassembly, and installation of the S-CO$_2$ recompression Brayton cycle at Sandia, obtaining safety approvals, and commissioning the loop at Sandia. This is expected to take about 6 to 8 months. The latter half of the year may then be used to explore the operational envelope of the S-CO$_2$ Brayton cycle and further develop and validate models of the loop.

Two 175-kWe Load Banks

With the most recent heater and recuperator upgrades, the S-CO$_2$ Brayton loop should be capable of producing relatively large amounts of electrical power (up to 80 kWe per turbomachine). To accommodate this large increase in power, two 175-kW load banks were ordered from Avtron LoadBank, Inc. These units were delivered to Barber Nichols and installed outdoors, adjacent to the Brayton cycle laboratory, where the electrical wiring and connections to the motor/generator controller were then completed. When shipped to Sandia, these load banks will have to be installed in Building 6630.

Two shutdown or overspeed resistors (OVRs) still need to be added to the loop. These resistors provide very low resistance that can be used to shut the turbomachine down in the event of an overspeed or during other conditions that demand rapid shutdown (e.g., failure of auxiliary equipment such as pumps, cooling flow, or instrumentation). The OVRs are currently scheduled for installation within the next 6 to 8 weeks.

Additional Evaporative Cooler (220-kW Rated) and Cooling Pumps

A second evaporative cooler was purchased and installed at the Barber Nichols test site. A photograph of the evaporative cooler is shown in Figure 0-6. This additional evaporator increases the cooling capability at the PCHE gas chiller to 440 kW based on the name plate rating. This upgraded cooling capability was first used with the main compressor Brayton loop tests performed in late November and early December 2010 to produce electrical power in the simple recuperated Brayton cycle configuration, allowing the production of electrical power in this configuration for the first time. These tests revealed that a larger water pump was required; therefore, a low-cost water pump was purchased and installed. Two other small water pumps were purchased to provide upgraded cooling flow for the motor controller box and turbomachinery housing, and also for cooling the Hydro-Pac hydraulic pump system. These pumps share their closed-loop water supply and cooling system with the PCHE gas chiller. Based on current testing, the available heat removal capability has been increased from 130–150 kW to about 280 kW. This is a substantial improvement, but will likely be one of the main limiting operating conditions while we continue testing at Barber Nichols.

Figure 0-6. Gen IV Brayton loop evaporative cooler.

The cooler has a name plate cooling capability of 220 kW.

Hydro-Pac Gas Scavenging Pump

Sandia purchased a hydraulically driven piston pump from Hydro-Pac, Inc., to more reliably reduce the rotor cavity pressure due to leakage, and to reduce windage and allow higher speed operation without overheating the turbomachinery. This single pump replaces the array of smaller, noisier, and frequently unreliable Haskel pumps that performed the same function in the previous configuration. The Hydro-Pac unit was received, installed, and first tested in April and May of 2011. This upgrade was largely responsible for the high shaft speeds and low windage losses achieved during this period. The Hydro-Pac pump and the Watlow® [4] heater controllers are shown in Figure 0-7.

Figure 0-7. The new Hydro-Pac scavenging pump and Watlow® heater controllers.

TESTING STATUS

Summary

A flow schematic of the Gen IV S-CO$_2$ split-flow (or recompression) loop as it was assembled in June of 2011 is illustrated in Figure 0-1. The two installed turbo-alternator-compressors (TACs) are shown in Figure 0-2. Previous testing and analysis of the S-CO$_2$ power system showed that, for initial testing, it is best to operate the loop as a simple heated recuperated Brayton loop rather than a split-flow loop, because it is easier to model and understand the loop's behavior. In addition, because only one compressor is used, the total flow rate through the heaters is lower, so it is easier to reach higher temperatures. With this in mind, this test series began by first running the Gen IV loop as a simple recuperated Brayton cycle. The Gen IV S-CO$_2$ Brayton loop was reconfigured to operate as a simple heated recuperated Brayton loop by removing the TAC-B turbomachine and blocking off the flow passages to it. Then, either the TAC-A or the TAC-B turbomachine was placed in the TAC-A location. This also allowed for an accurate comparison with the results from tests performed in FY2010.

A simplified schematic of the simple heated recuperated configuration flow loop with the upgrades that were commissioned and installed in FY2011 is shown in Figure 0-1, above. Figure 0-1 also shows the locations of the temperature and pressure sensors. Note the numbers (shown in green in the figure) beginning with the value 100 at the turbine inlet, 200 at the turbine outlet, increasing around the loop, and ending with 600 at the heater outlet. These identifiers serve as a legend for interpreting the data presented later in this section.

Two series of tests were performed: 1) the first running the main compressor turbomachine (TAC-A), and 2) the second running the recompressor turbomachinery (TAC-B) after removing TAC-A and installing TAC-B in its place. Tests with TAC-A provided the first confirmation that the Hydro-Pac scavenging pump system was operating properly and was able to reduce the rotor cavity pressure to 1.4 MPa (200 psia). These tests also revealed that the Hydro-Pac pump caused mass flow oscillations with each piston stroke changing the compressor inlet fluid density. This was corrected by rerouting the Hydro-Pac reinjection point to just before the gas chiller.

With the TAC-A main compressor unit operating, break-even conditions were approached near 500°F, although electrical generation was not attempted because of the unfavorable flow conditions observed at this point. At the conclusion of the tests, the TAC-A gas foil thrust bearing was damaged, most likely because of a poorly balanced thrust load towards the turbine (previously observed in FY2010), and because the turbine bypass valve was opened at the end of the test, which further misbalanced the thrust load. The turbocompressor was then switched out to TAC-B, and subsequent tests used the larger compressor found on this alternate unit.

Testing with TAC-B proved very successful. The mass flow oscillation issue was indentified and addressed, as detailed below. Free from the flow oscillations, the test conditions were allowed to proceed to the highest turbine inlet temperatures (TIT), speeds, and power generation yet achieved on this system, all while maintaining the lowest bearing temperatures. Conditions peaked at a TIT of 650°F and a speed of 51,000 rpm, resulting in a generation of 20 kWe. At this

point, a component of the motor controller box malfunctioned, and the system was shut down for repairs. (This has since been fixed).
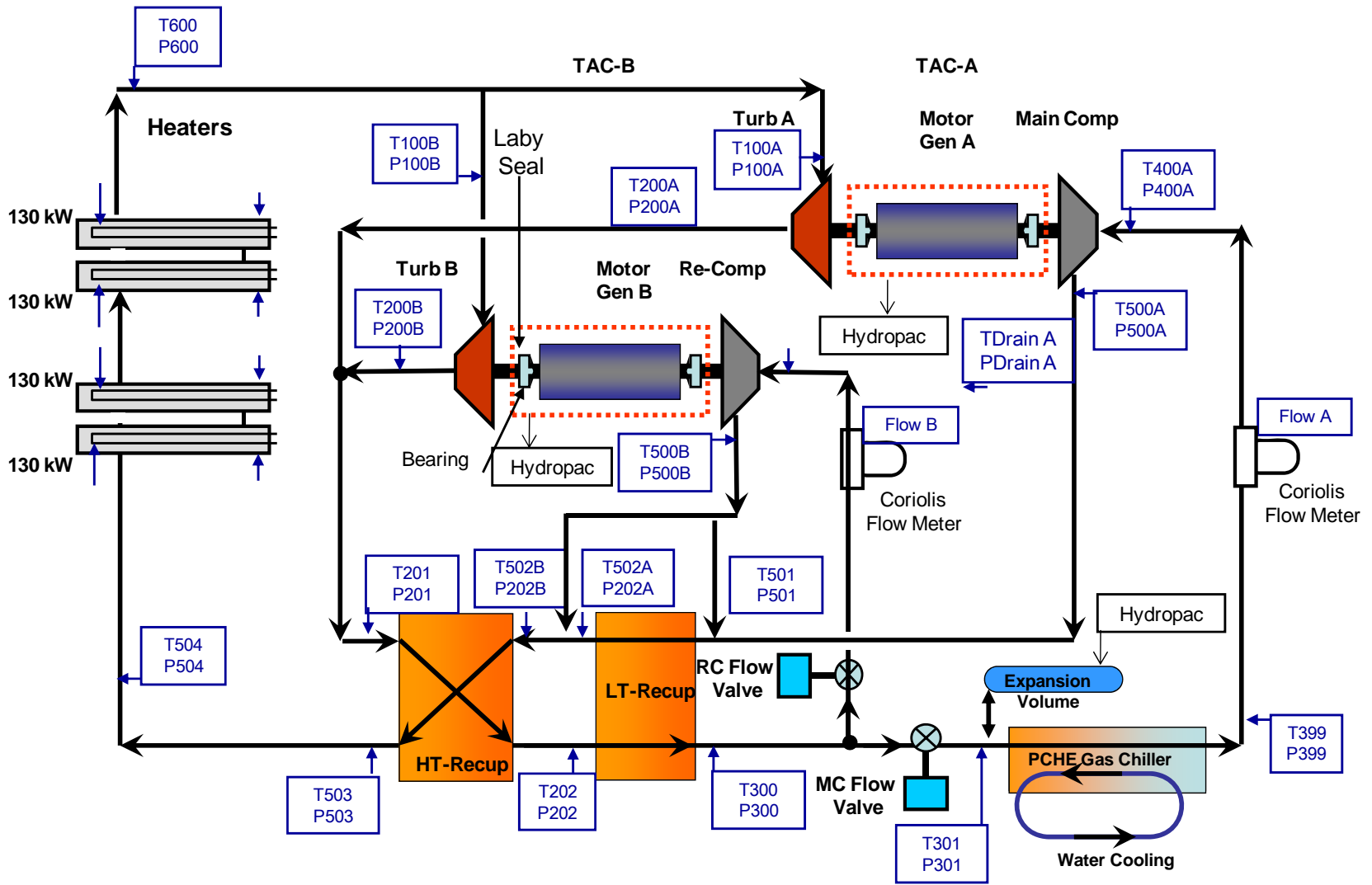
Figure 0-1. Flow schematic of the Gen-IV 520-kW split-flow Brayton cycle.

The blue outlined boxes mark the temperature and pressure labels and the locations of the sensors.
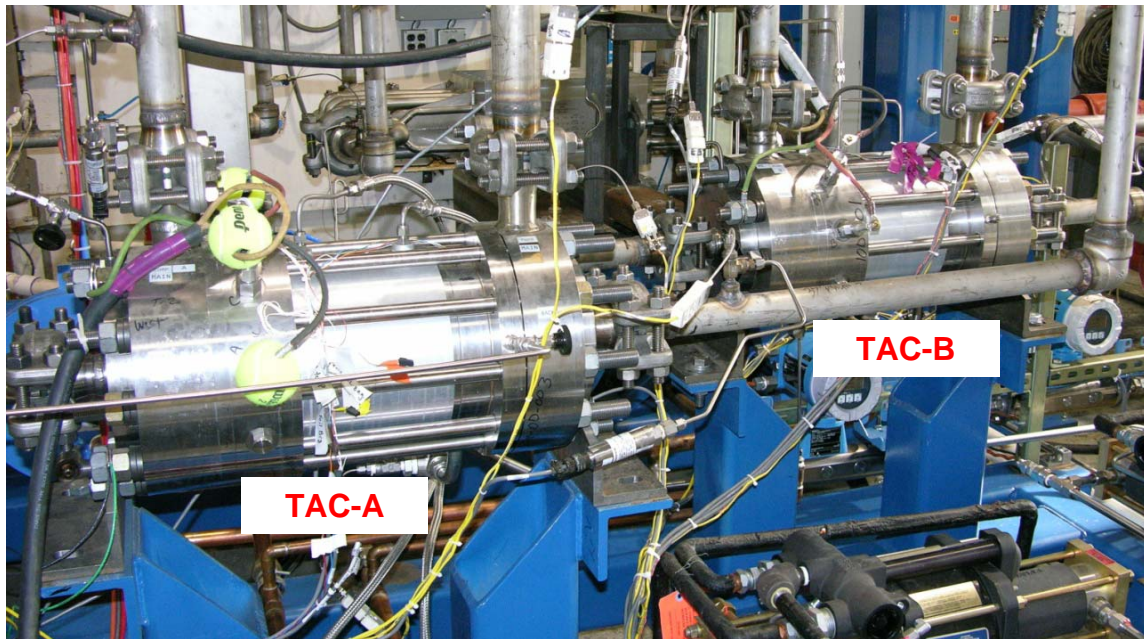
Figure 0-2. TAC- A and TAC-B installed in the split-flow recompression configuration.

These test runs provided a wealth of new insights into the functioning of the turbine, the generator, and the PCHEs manufactured by Heatric. In essence, the testing confirmed the that 1) the new hardware upgrades significantly increase the operational performance of the loop and the turbomachinery, 2) all upgrades operate and function seamlessly with the newly updated and expanded control system, and 3) the system operational limits are largely related to the support hardware (e.g., evaporative cooler limits, motor generator circuitry, water pumps)—and not the turbomachinery.

TAC-A Brayton Cycle Testing

Five periods of testing were performed with the main compressor turbomachinery (TAC-A). This section focuses on a run performed on June 22, 2011, which approached break-even power production conditions.

Testing started off in the simple Brayton cycle configuration by motoring the compressor to 30,000 rpm with the turbine bypass valve open. The procedure then closely followed the cold-startup process developed in earlier work: the bypass valve was slowly closed down while simultaneously increasing the heater power level to increase the temperature of the gas supply to the turbine. The Hydro-Pac unit was also motored to draw leakage gas from the rotor cavity and pump it back into the system (through valve C1, as illustrated in Figure 0-1). The TAC motor power slowly decreased with the rising turbine inlet temperature and bypass valve closure.

One observation of this test was the persistent mass flow oscillations (with variations of approximately 40–50% of the mean flow rate) during operation of the Hydro-Pac. Prior to its installation and other recent upgrades, the loop used less-capable scavenging pumps and operated with steady mass flows, generating electricity at the same compressor inlet conditions without issue.

A variety of small tests were performed that confirmed that these oscillations were caused by compressor inlet density variations caused by the piston stroke in the Hydro-Pac. The flow oscillations became progressively worse as the bypass valve was drawn down. This continued even as the turbine inlet temperature was heated to 500°F, and break-even power generation conditions were approached near 8000 seconds (s) into the test. At this point, the compressor inlet density had reached 560 kg/m^3 (35 lb/ft^3) and conditions were comfortably supercritical as judged by the temperature and pressure; however, the mass flow rate was still undergoing oscillations ranging from 0.5 to 1.0 kg/s. Because of these undesirable conditions, it was decided not to cross over into power production during this run. Figure 0-3 illustrates the T-S diagram for the system near the break-even point at 8000 s.
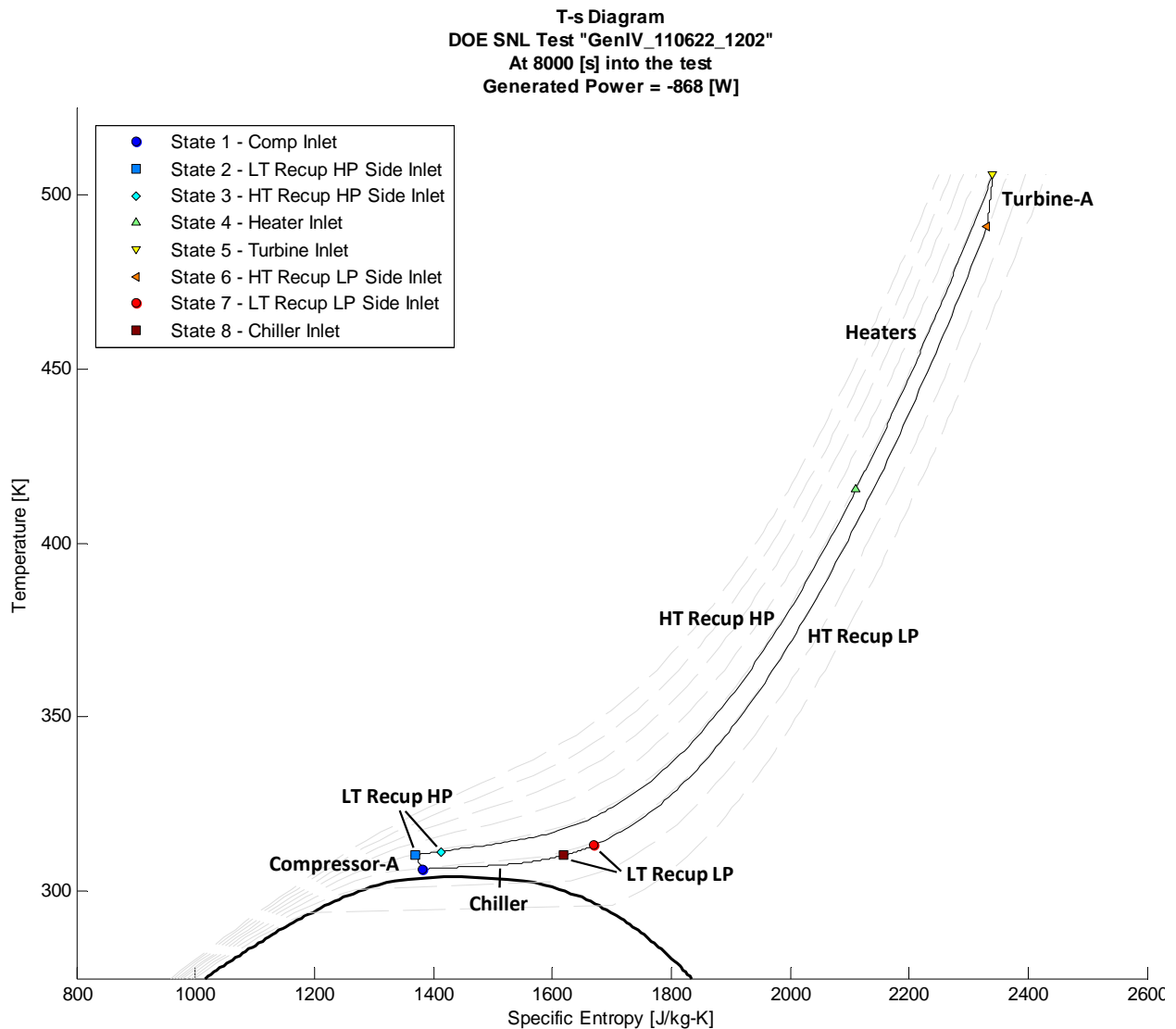
Figure 0-3. T-S diagram for the simple recuperated Brayton system using TAC-A at 8000 s into the test.

After a short investigation, it was determined that this mass flow/density oscillation effect was caused the reintroduction of the Hydro-Pac outlet flow into the main system flow directly before the compressor inlet. This issue had not been observed in the previous configuration using the less-powerful Haskel scavenging pumps. Temperature oscillations caused by each stroke of the Hydro-Pac scavenging pump were measured at the compressor inlet. As illustrated in Figure 0-3, a small change in temperature near the critical point results in a large change in entropy and density at constant pressure (near 7.7 MPa). This density change naturally resulted in a mass flow rate variation within the compressor.

This issue was addressed by rerouting the Hydro-Pac outlet to a point upstream of the PCHE gas chiller (illustrated in Figure 0-1 as the path connecting to valve C2). The two streams would then have a chance to be thoroughly mixed and cooled within the microchannels of the PCHE before entering the compressor, ensuring stable single-phase inlet conditions. After making this change to the system plumbing, the flow oscillations were eliminated.

Unfortunately, during the cooldown process, the gas foil thrust bearings were damaged before we had the chance to run more power generation tests. The bearing damage occurred when the turbine bypass valve was opened after the heaters were turned off to avoid the flow reversal in the loop. This likely caused a sudden change in thrust load on the bearings as well as power and bearing temperature spikes, indicating a bearings failure. This same type of bearing failure was observed before in this TAC, which always failed on the turbine side of the thrust bearing. We believe the failure is due to poorly balanced thrust. It can be corrected by increasing the size of the "cutouts" in the turbine wheel. At the current time, other changes are planned that would also alter the thrust load, including replacing the main compressor wheel with the recompressor wheel. Because the TAC-B unit appears to be well balanced, we are not planning on increasing the size of the "cutouts" at this time.

While the TAC-A unit awaited repairs, the turbocompressor was switched out to TAC-B, and testing continued with this larger compressor.

TAC-B Brayton Cycle Testing

Five tests were run using TAC-B. Each test or run generally lasted several hours; with post-test analysis, it was generally possible to perform only one or two tests per day. This section of the report focuses on the experiment that was the most successful from the standpoint of peak steady-state electrical generation. Data from this run, made on July 14, 2011, is presented in Figures 3-4 through 3-10 (TAC-B shaft speed and power, loop temperatures, mass flow rates, loop pressures, bearing temperatures, turbine/compressor characteristics, component power balances, and heater temperatures, respectively), and provide an enormous amount of information about the test run from start to finish. A few brief comments are provided in the text or in the caption for each figure. The locations of the sensors that correspond to the data in the figures (e.g., T504 in Figure 0-5) are shown in the flow schematic in Figure 3-1, above.
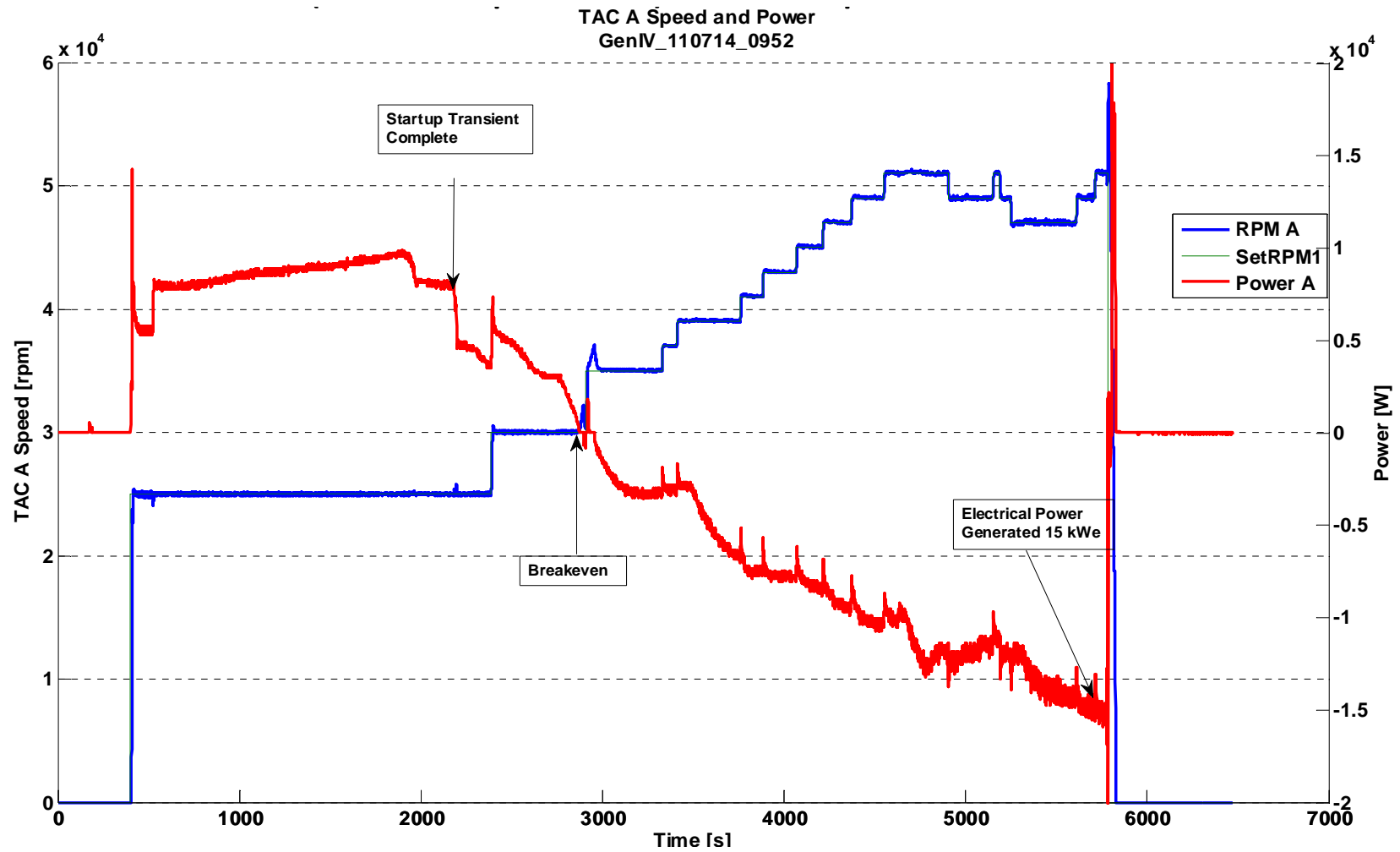
Figure 0-4. TAC-B shaft speed and power for DOE SNL Test "GenIV_110714_0952."

**Temperature and TAC A Speed
GenIV_110714_0952**
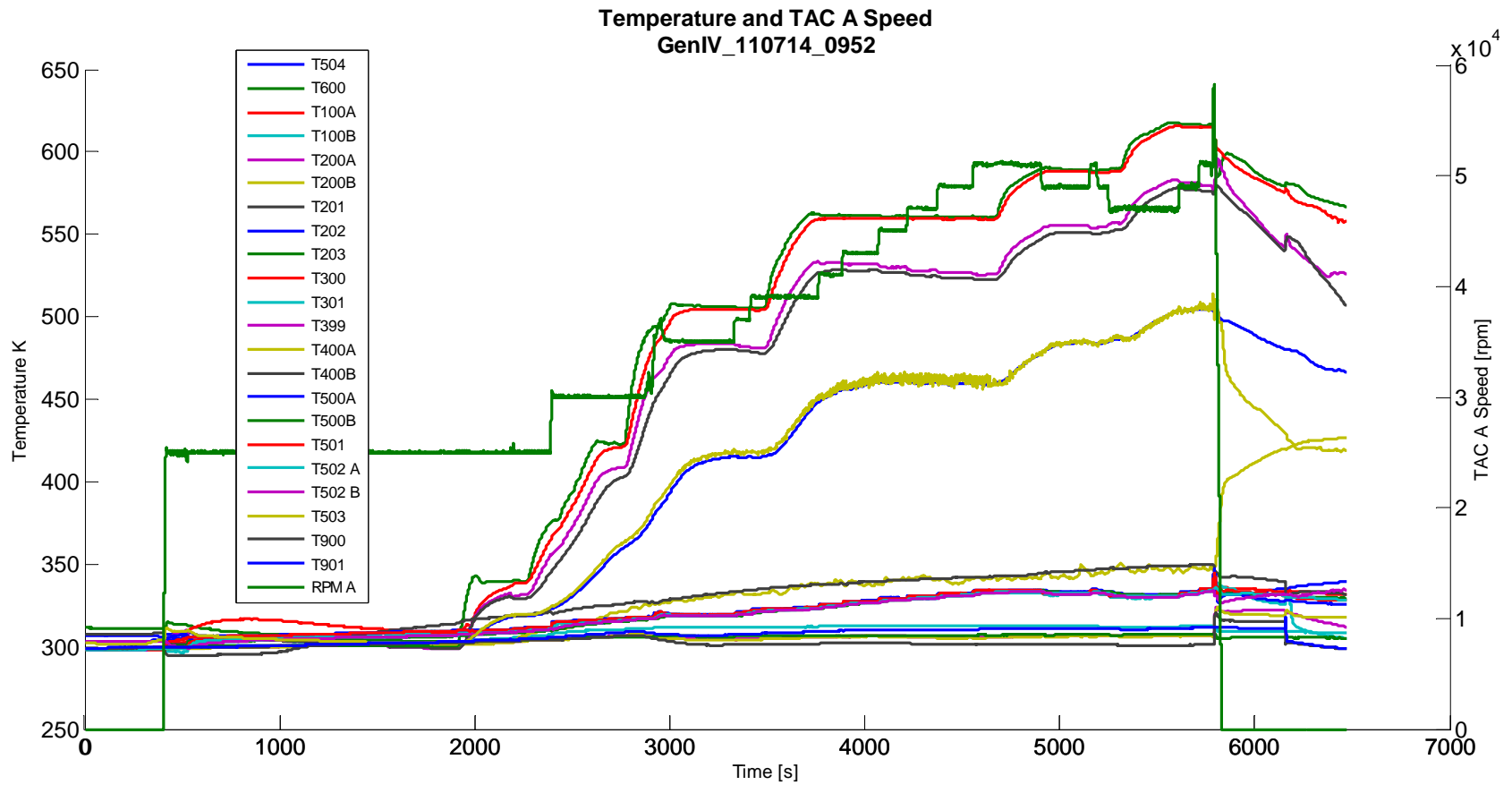
Figure 0-5. TAC-B loop temperatures for DOE SNL Test "GenIV_110714_0952."
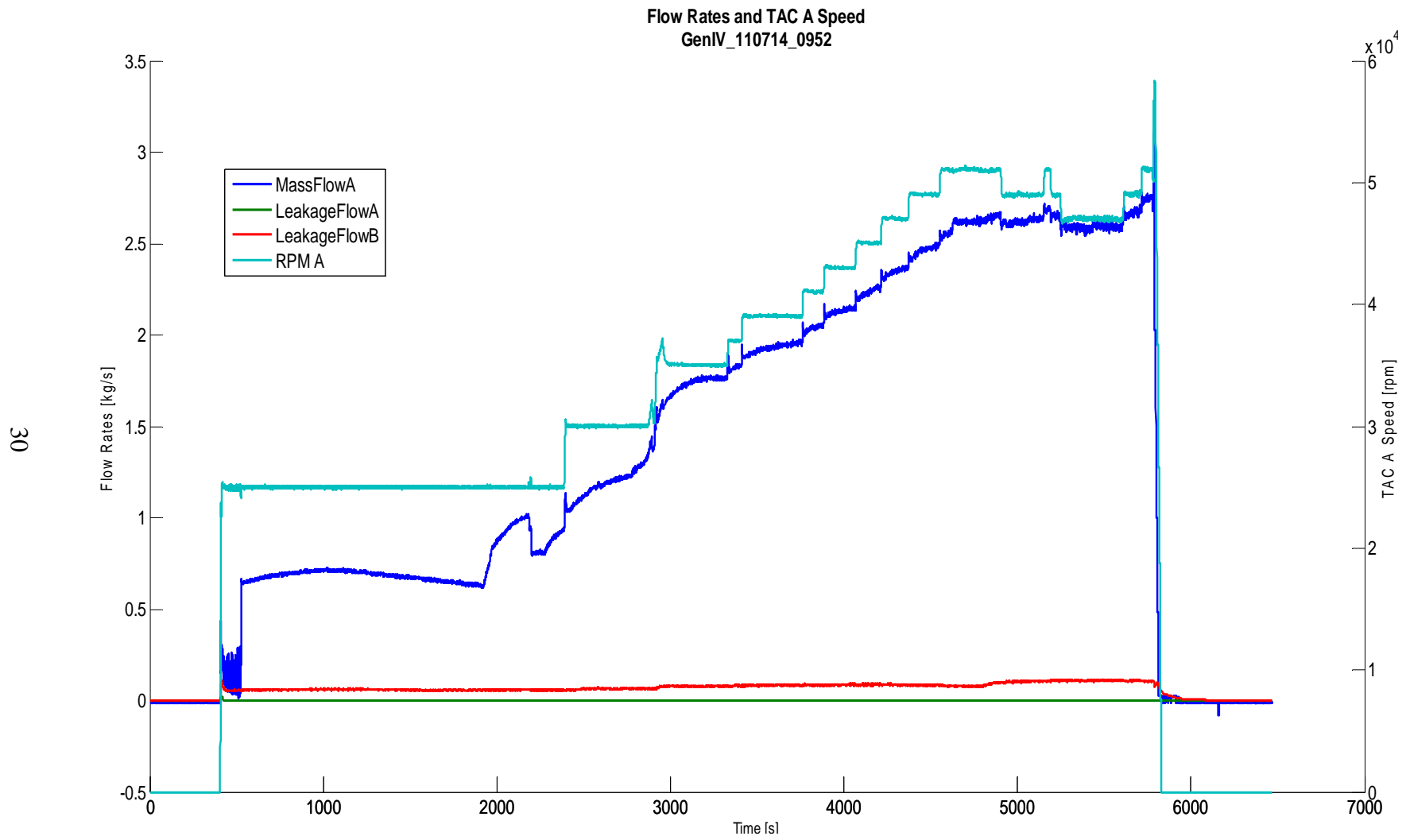
Figure 0-6. TAC-B mass flow rates for DOE SNL Test "GenIV_110714_0952."
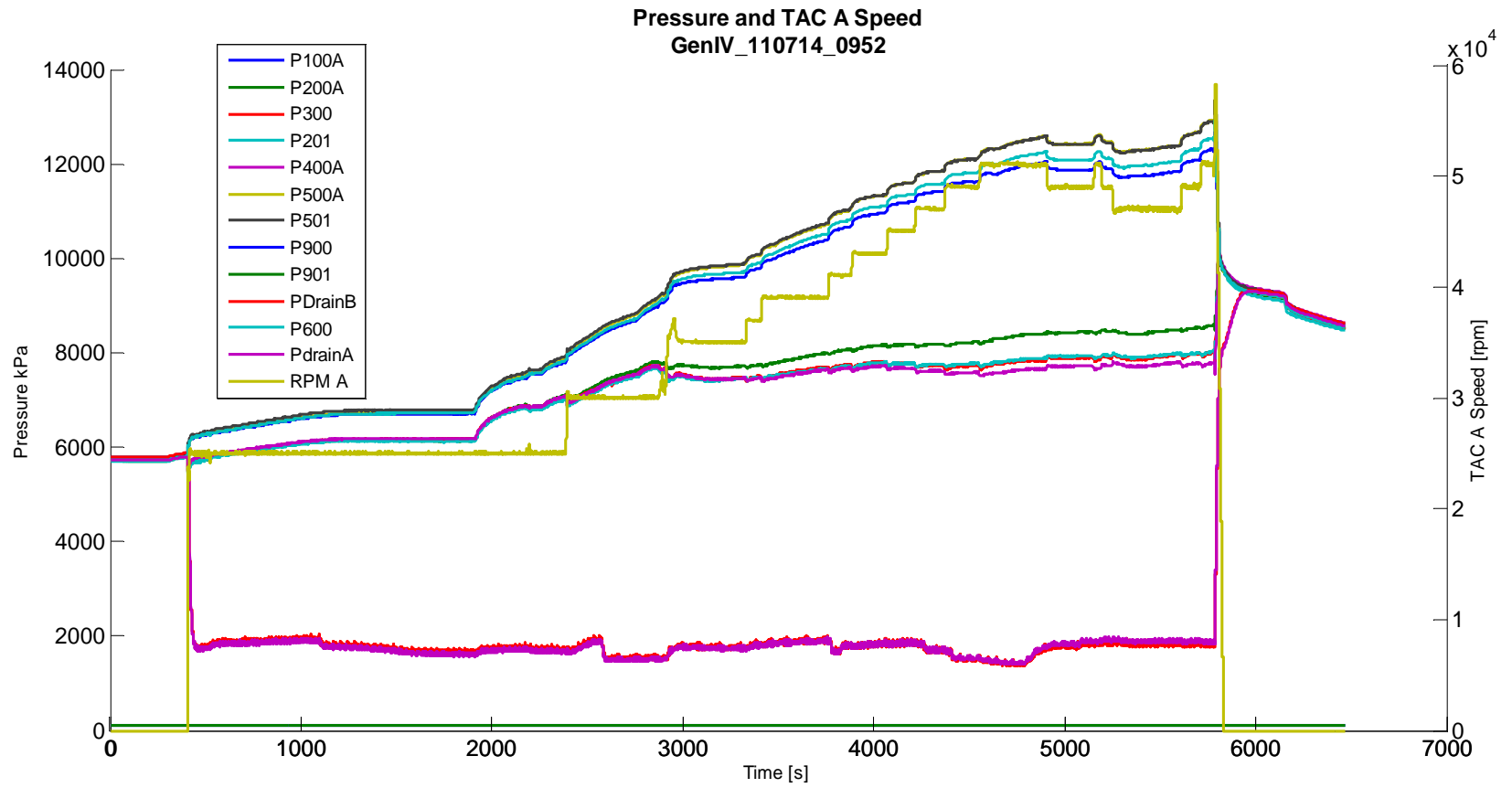
Figure 0-7. TAC-B loop pressures for DOE SNL Test "GenIV_110714_0952."
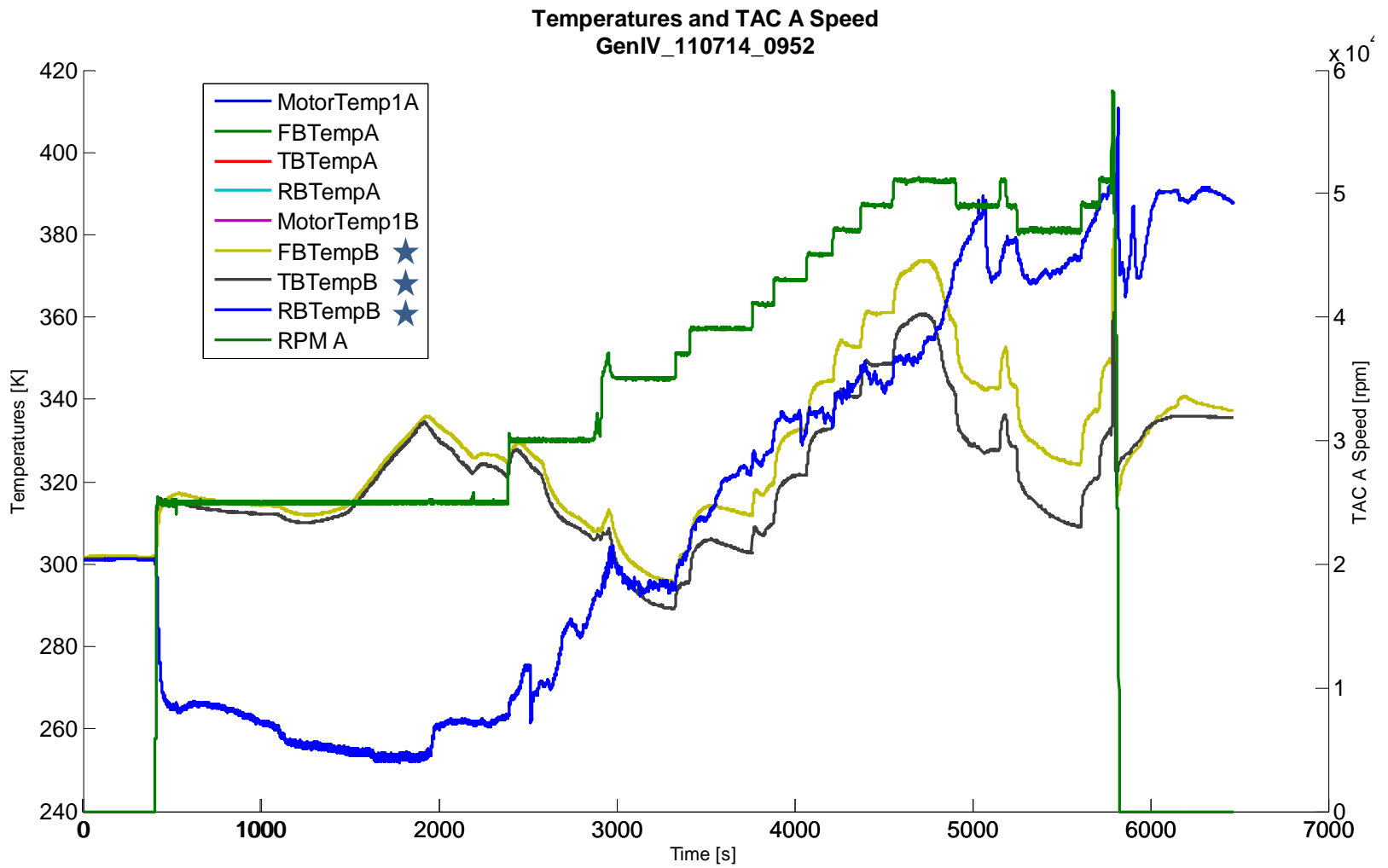
Figure 0-8. TAC-B bearing temperatures for DOE SNL Test "GenIV_110714_0952."
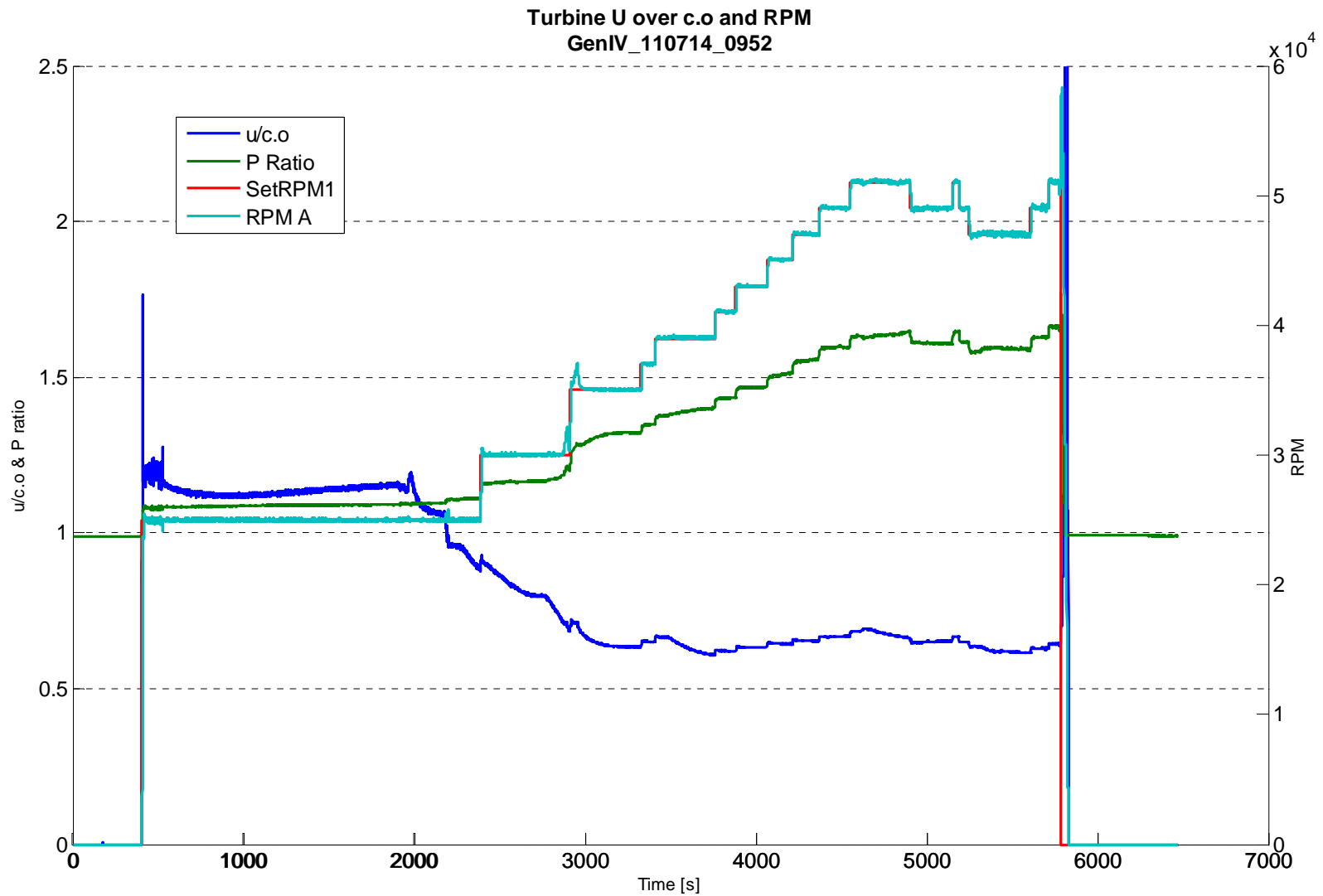
Figure 0-9. TAC-B turbine/compressor characteristics (u/c$_o$, pressure ratio, and rpm) for DOE SNL Test "GenIV_110714_0952."
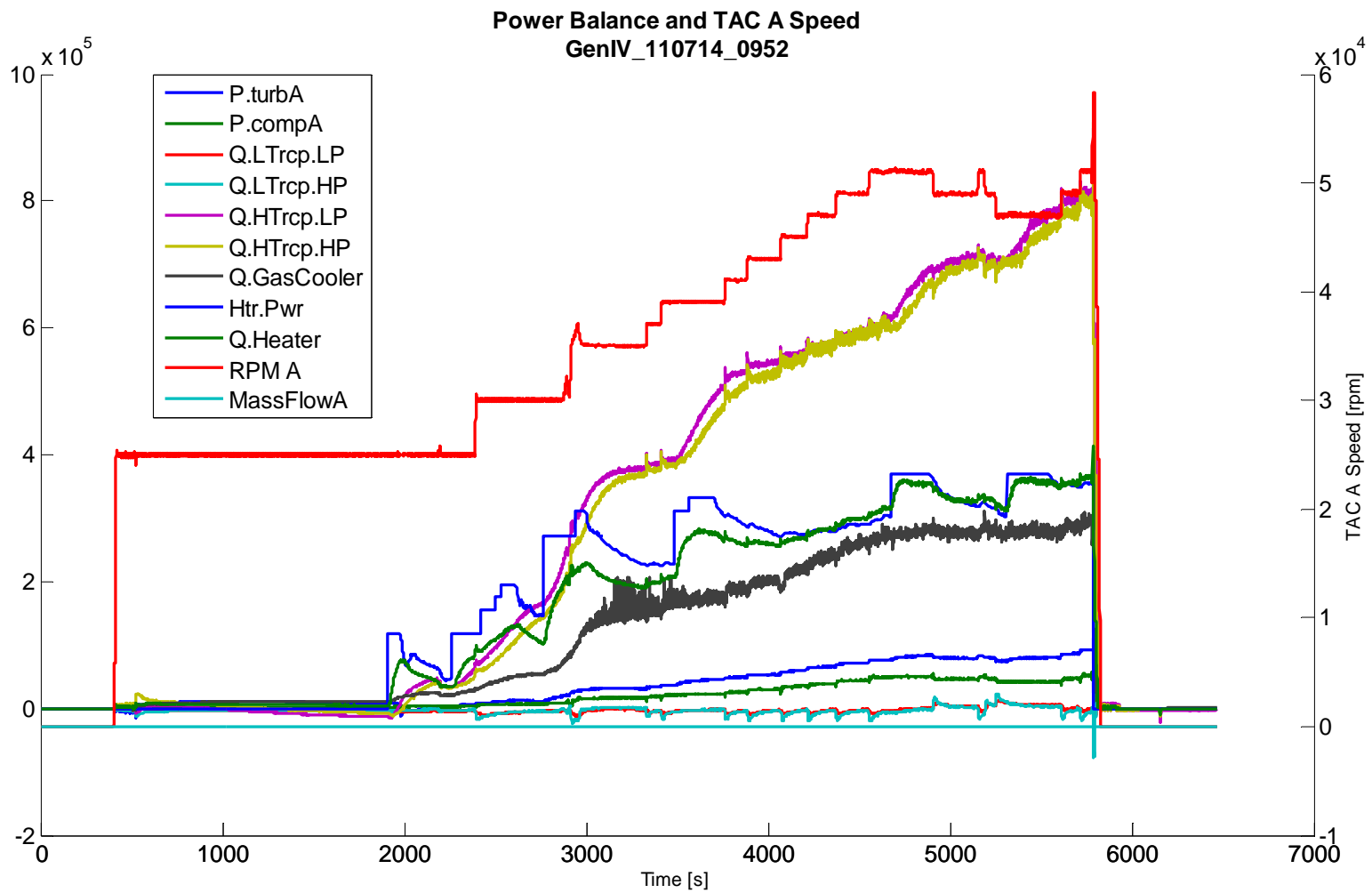
Figure 0-10. TAC-B component power balances for DOE SNL Test "GenIV_110714_0952."
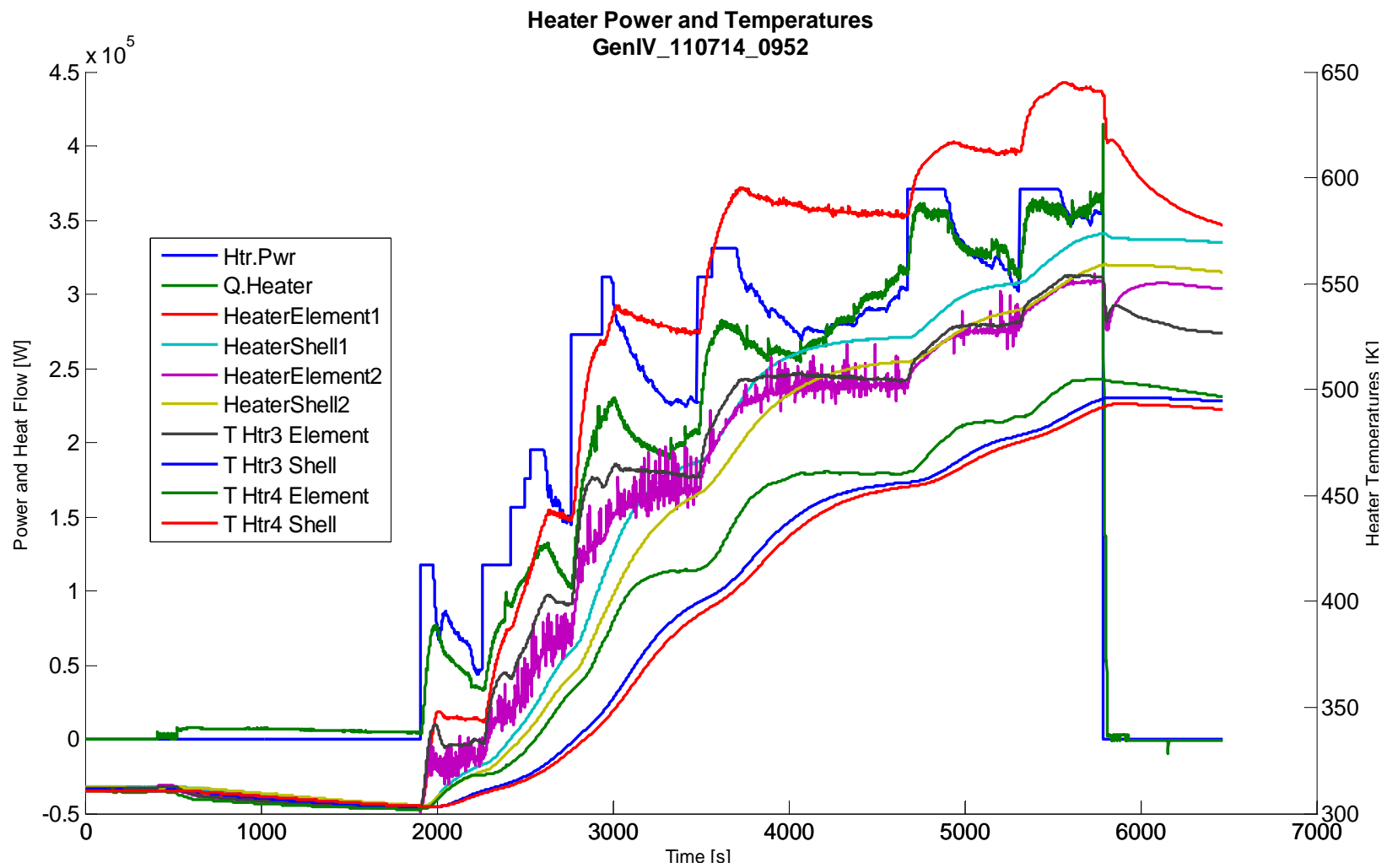
Figure 0-11. TAC-B measured heater temperatures for DOE SNL Test "GenIV_110714_0952."

The July 14, 2011, test began from cold startup conditions (300 K), motoring TAC-B at 25,000 rpm with the turbine bypass valve fully open (see Figure 0-4). The heaters were turned on to quickly heat turbine inlet conditions to 340 K (150°F) by 2200 s, as illustrated in Figure 0-5. At 2200 s, the turbine bypass valve was gradually drawn to a fully closed position to force all flow to pass through the turbine in the correct direction. The turbine bypass valve closure shows up as a motor power reduction (at 2200 s, Figure 0-4), a mass flow rate reduction (see Figure 0-6), and a slight spike in rpm (at 2200 s). The compressor inlet density at this time was around 240 kg/m^3 (15 lb/ft^3), which is near the recompressor design conditions. Heating of the system then continued at 30,000 rpm with motor power dropping until break-even conditions were achieved just before 3000 s at 500 K (440°F). From this time forward (>3000 s), the density was near 0.55 kg/liter, which is very close to the design condition for the main compressor.

Heater power was then increased to drive up the temperature in steps from 500 to 590 K (600°F), and shaft speed was incrementally increased from 30,000 to 50,000 rpm (see Figure 0-4). The ability to reach 50,000 rpm and to operate for long periods of time at high speed was made possible during these runs for the first time only by the performance of the Hydro-Pac pump, which kept rotor cavity pressure comfortably below 2 MPa (290 psi) throughout testing (see Figure 0-7). Bearing temperatures never exceeded 400 K (260°F), well below maximum design temperatures (see Figure 0-8), and power consumed by windage losses dropped considerably. This drove electrical power, as transmitted by the motor/generator controller unit, to new record highs.

Note that electrical power output was measured two different ways: 1) using a Yokogawa WT1600 Digital Power Meter attached directly to the generator of TAC-B (see Figure 0-12), and 2) after being switched, using the solid-state insulated gate bipolar transistors (IGBTs), and filtered through the motor/generator controller electronics. The latter value is reported as the red line in Figure 0-4. The motor/generator controller electronics were observed to report an average load power of about 70% of the direct measurement (as seen by the Yokogawa meter), suggesting large inefficiencies in the controller box at present. In contrast, when the motor generator was in the motoring mode, the reported difference in power between the controller circuits and the direct measurement was 88–89%. This indicated greater losses in the power generating circuitry than the motoring circuitry. Currently, this difference is believed to have been caused by an inappropriately sized coil/filter.

Next, at approximately 5000 s into the operation, the speed was brought down in steps to 46,000 rpm to gauge the response of power produced to shaft speed at a turbine inlet temperature of 590 K (600°F). As indicated in Figure 0-4, the effect was very small in the range examined. Figure 3-7, however, shows a decrease in the turbine tip speed to spouting velocity ratio (u/c_o) as speed is dropped. This indicates that the turbine speed is heading towards slightly less favorable operating conditions and should instead be increased for optimal performance and maximum power output at this turbine inlet temperature.
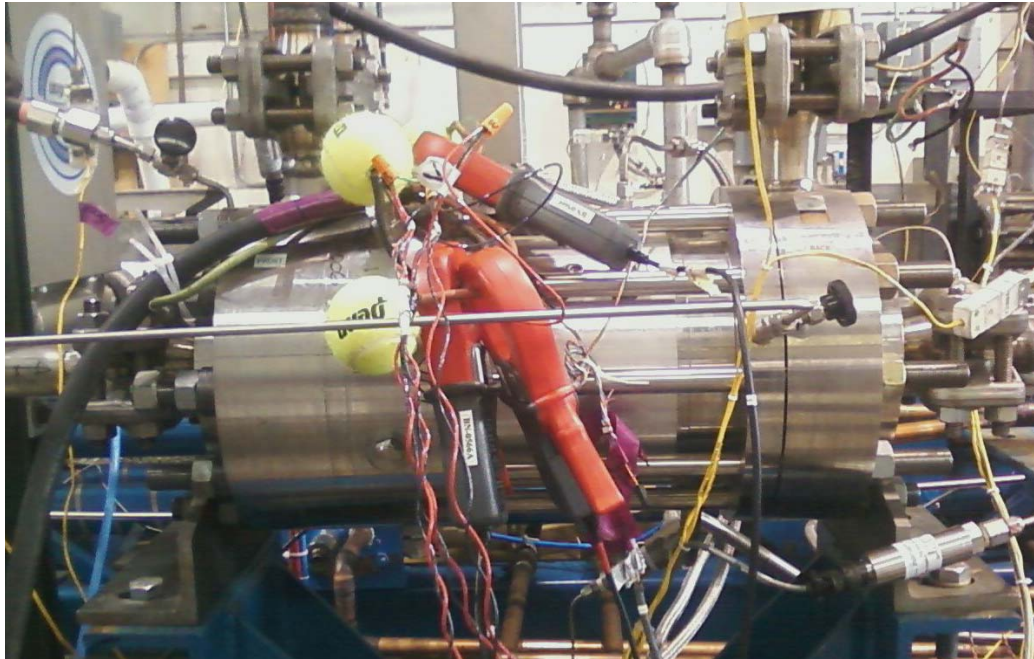
Figure 0-12. Yokogawa WT1600 Digital Power Meter attached to TAC-B.

Finally, the turbine inlet temperature was increased to 615 K (650°F) and the speed was brought back up to 51,000 rpm, driving the compressor outlet pressure above 12.4 MPa (1850 psi) (see Figure 0-7) to a pressure ratio above 1.65 and causing the electrical power generated to approach 16 kWe. Measured at the Yokogawa power meter, this power exceeded ***20 kWe.*** For an applied thermal power of 370 kW, this represents an achieved cycle efficiency greater than 5%. The diesel generator rented for this series of tests was capable of producing only 390 kW, so it was not possible to increase turbine inlet temperature much further. Figure 0-8 shows that, at peak conditions, upwards of 800 kW of power were transferred in the newly installed HT recuperator, more than doubling the power input by the heaters. Other information regarding the heaters is presented in Figures 3-8 and 3-9. The bearing temperature is shown in Figure 0-8, and the mass flow rate is shown in Figure 0-6.

For the majority of the test run, however, the hot and cold streams in the LT recuperator were observed to approach each other before exiting the HT recuperator a condition commonly referred to as 'pinching', which meant that the entire LT recuperator provided no benefit. In fact, the LT recuperator is shown to transfer 'negative' power, actually precooling the CO_2 flow between the compressor outlet and the HT recuperator. Power transferred does briefly spike above zero in two instances towards the latter part of the test.

A detailed analysis of the heat exchangers and their performance during this experiment is presented in Section 3.4. It is clear that, in this configuration and at these conditions, the loop is over-recuperated, and the LT recuperator serves only as an unnecessary pressure drop. Moving to the split-flow configuration in future runs while using higher power input will allow the test to unlock the full potential of both recuperators and radically increase power conversion efficiency.

A temperature-entropy (T-S) diagram of the CO_2 Brayton cycle operation from the period of peak power generation (5770 s into the test) is provided in Figure 0-13. The figure shows the recompressor (TAC-B) operating far from its design point. TAC-B is designed to operate at 75,000 rpm and pump 2.5 kg/s (5 lb/s) of gas phase CO_2 at 340 K (150°F), at 7.75 MPa (1125 psi) and approximately 250 kg/m^3 (15 lb/ft^3), to a pressure ratio of 1.8. Here it is seen to produce its design flow rate of 2.5 kg/s, and nearly its design pressure ratio, even though it is operating at only 2/3 of its intended speed, at far cooler and more dense inlet conditions than its design point. In fact, at 305 K and 400 kg/m^3, the recompressor in this test operates at very nearly the conditions expected of the smaller main compressor. This indicates that a larger compressor wheel such as that found on the recompressor may be more favorable for use at the main compressor on TAC-A as well, and may achieve the desired flow rate and pressure ratio at lower speeds, further reducing turbomachinery windage. A larger wheel would also help the main compressor overcome the main turbine in opposed flow conditions at cold startup. This may become an even greater concern as the facility moves towards the split-flow operation.

Figure 0-10, above, provides a revealing look into the inefficiencies in the process of power generation for this system. At peak conditions, the turbine is receiving close to 92 kW, as measured by the mass flow and change in enthalpy from inlet to outlet. Meanwhile, the compressor is consuming around 52 kW, leaving 40 kW of net work that can be converted from thermal to mechanical energy. Unfortunately, only 20 kW is being converted to electricity, of which 16 kW is transmitted to the load banks. Using previously developed correlations for windage and other best practice estimates, it is likely that 9 kW of loss is due to frictional effects and 11 kW to thermal losses. Figure 0-14 gives a breakdown of these contributions. Thermal loss can be chiefly attributed to heat transfer from the turbine through the TAC pressure vessel and into the water cooling lines in the jacket of the TAC housing. Other natural convection and radiative losses are also present, especially at high temperature. Plans to alleviate this in future runs will focus on better insulation of the TAC housing from its hot turbine side nozzle and shroud, and improved piping insulation in general, which must wait until the piping sizes have been increased.

As noted, only 70–75% of the generated power was actually transmitted to the load banks. This is due to considerable losses within the motor/generator controller electronics and windage. As a result of these tests, it was noted that an inductor coil used for filtering the incoming signal was not rated for the design conditions of this test. The coil will be replaced. Swapping out this unit should have an immediate impact on future results. Still, some of these losses are an unavoidable effect of switching in the electronics. It is anticipated that this efficiency will only reach 88–90% at maximum.
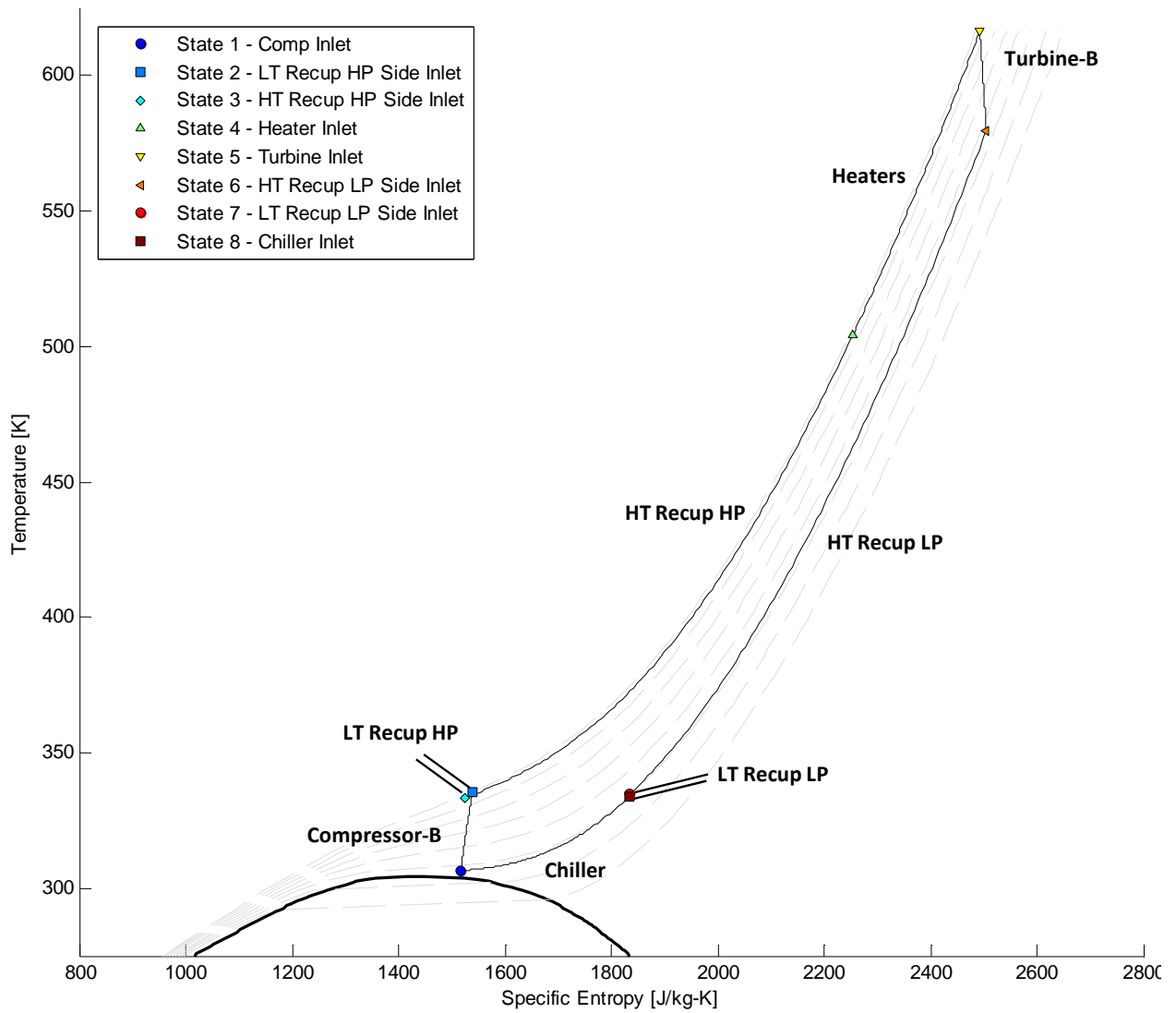
Figure 0-13. T-S cycle diagram while generating 20 kWe with the recompressor.
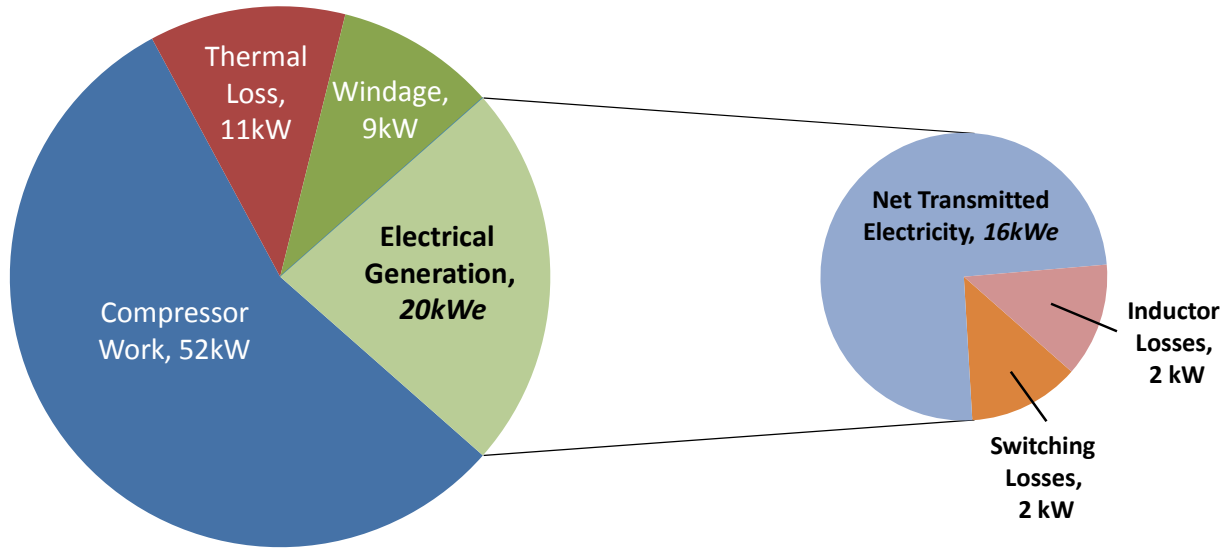
Figure 0-14. Breakdown of power losses during recompressor electrical generation at 20 kWe.

While the facility was running at high speed and high temperature, producing 20 kWe, the test ended abruptly when the motor/generator controller failed, causing the load bank to disconnect from the turbo-generator. This caused the shaft speed to climb to its 'natural' zero-load speed near 60,000 rpm, before slowly coasting back down to 0 rpm. The "zero-load" speed is the shaft speed where the power consumed by the compressor and windage just equals the motive power generated in the turbine. Figure 0-15 shows rotation speed in blue and the commanded speed in green. These lie on top of one another for the entire run, excluding the free-wheeling portion at the end of the test. Although unplanned, the ability of the system to self-brake and return to zero power and speed helps to illustrate its inherent safety and stability.

Finally, note that the compressor inlet density ended up at 400 kg/m^3 (25 lb/ft^3), as shown in Figure 0-16. Note that this final density value is substantially larger than the density at the start of the test, despite the fixed mass of CO_2 in the loop. As the heaters became engaged, the 'hot' side (near the heaters and turbine) became less dense, displacing CO_2 towards the 'cold' side and increasing density at the compressor inlet. This means that, when performing the initial system fill, it is difficult to pinpoint the CO_2 fill mass that will eventually provide desired compressor inlet conditions at a desired turbine inlet temperature, except by trial and error. The sensitivity of compressor inlet density to hot-side temperature has increased with the addition of the two new heaters. This issue should be addressed by purchasing and installing supplemental expansion tanks for the cold-side of the loop to balance the hot-side volume increase introduced by the heaters.
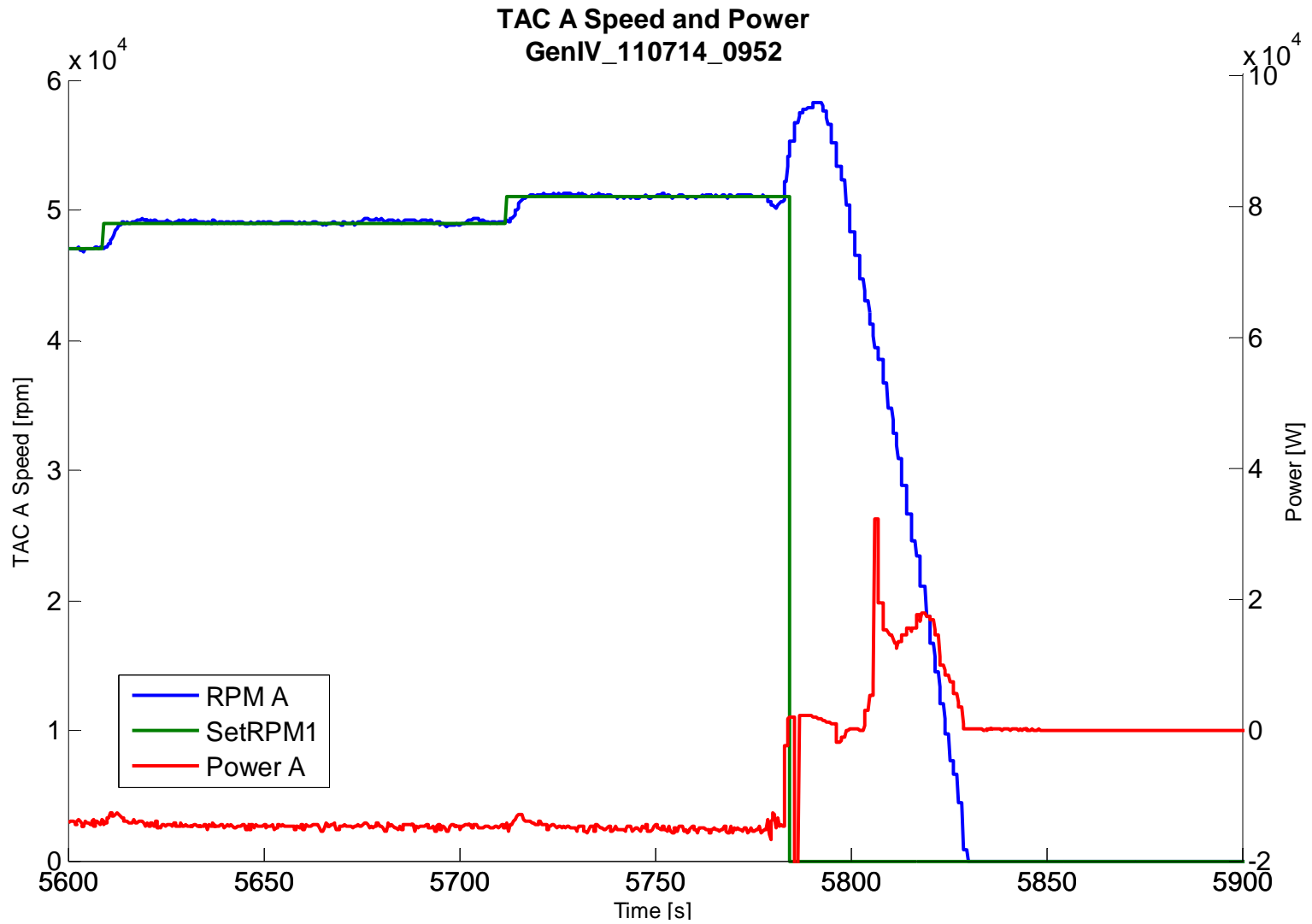
Figure 0-15. Measured data during an unplanned turbine trip and coastdown at 20-kWe electrical generation.
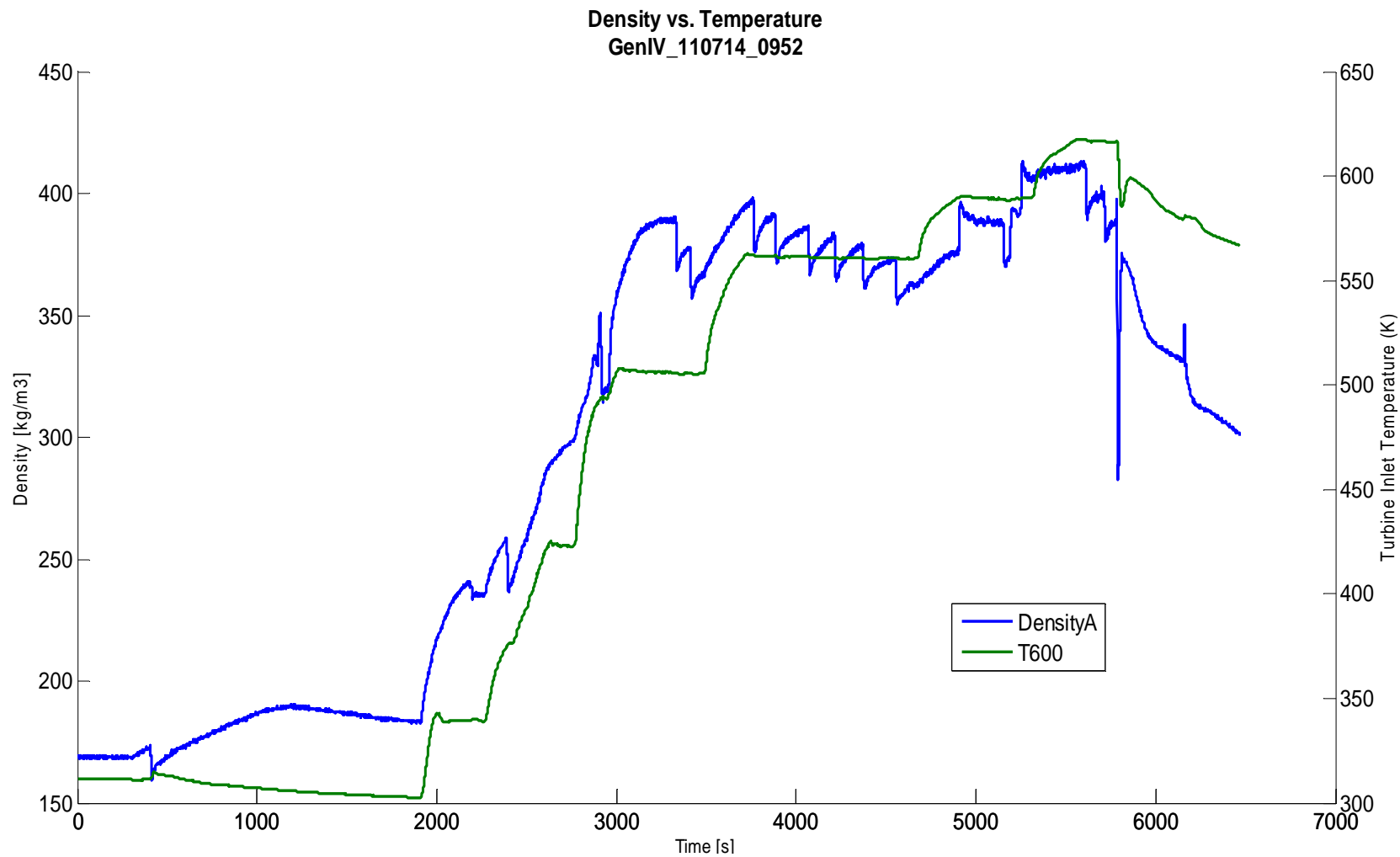
Figure 0-16. Measured compressor inlet density versus loop hot-side temperature during the test run.

Performance of the Printed Circuit Heat Exchangers (PCHEs)

The HT and LT PCHEs and the PCHE gas chiller currently installed in the DOE Gen IV loop are sized for operation in both the simple and split-flow recuperated Brayton cycle configurations with maximum expected operating conditions, as summarized in Table 0-1. Because recent tests were carried out well below the design conditions with respect to temperature and power levels, and because the tests were performed in a simple recuperated Brayton cycle (not the recompression cycle), a pinch point has been observed in the HT and LT recuperators. The pinch point occurs because the heat capacity of the high-pressure fluid is higher than in the low-pressure leg of the recuperator (by almost a factor of 2). The existence of this pinch point was expected due to the limited temperatures and power levels used in the recent testing. A second type of pinching can occur in the lowest-temperature recuperator and/or gas chiller due to the rapidly changing properties of the fluid properties of the CO_2 when it is near the critical point.

**Table 0-1. Design Conditions and Estimated Conductance-Area Product (UA)
of the Gen IV Test Loop PCHEs.**

	Hot Side	Cold Side
HT Recuperator		
Fluid	CO_2	CO_2
Temperature (in/out) (K)	752.32 / 408.87	387.98 / 703.87
Inlet Pressure (MPa)	7.977	13.76
Pressure Drop (kPa)	82.74	103.4
Flow Rate (kg/s)	5.761	5.715
Heat Transfer (kW)	2313	
Approximate UA (kW/K)	56.49	
Approximate Hydraulic Diameter (mm)	1.0607	
Approximated Flow Length (m)	1.196	
	Hot Side	**Cold Side**
LT Recuperator		
Fluid	CO_2	CO_2
Temperature (in/out) (K)	408.87 / 333.094	324.761 / 387.98
Inlet Pressure (MPa)	7.894	13.84
Pressure Drop (kPa)	124.1	82.74
Flow Rate (kg/s)	5.761	3.45
Heat Transfer (kW)	610.46	
Approximate UA (kW/K)	33.98	
Approximate Hydraulic Diameter (mm)	0.887	
Approximated Flow Length (m)	0.53	

A description of the pinching phenomenon as observed in these tests is provided here to illustrate its nature. The effect of pinching is often mentioned in many reports, and its occurrence is the reason why the recompression cycle was invented (to avoid the pinch). These tests provide the first opportunity to link observed pinching behavior with experiment measurements in the S-CO$_2$ system. Although the PCHE pinched, it caused no issues with the operation of the Gen IV loop. The pinch point phenomena in the recuperators will disappear at higher levels of temperature and power, and when the loop is operated as a recompression cycle. In fact, the pinch was beginning to disappear between 5000 and 5700 s as a small amount of heat transfer was occurring in the LR recuperator, as shown in Figure 0-10 and again in Figure 0-18, which plot the measured heat transfer in the HT and LT recuperators.

As illustrated in Figure 0-1 and Figure 0-1, above, the HT and LT recuperators are counter-flow heat exchangers connected in series for the simple heated recuperated Brayton cycle testing. This means that they both have identical mass flow rates during operation in the simple recuperated Brayton cycle configuration. Therefore, the heat exchangers can be considered one long heat exchanger that is "used" from the hot-stream inlet side to the cold-stream inlet side.

A pinch point is a location where the two fluid stream temperatures approach each other, resulting in relatively little driving temperature difference to transfer heat between the streams. A pinch point can occur under two general conditions, as follows: 1) When the hot stream temperature reaches the inlet temperature of the cold stream indicating that the heat exchanger is larger than necessary for that operating condition. This generally occurs in a simple recuperated Brayton cycle. 2) When the temperature and pressure dependence of the fluids' specific enthalpy causes the two fluid temperatures to approach each other at temperatures higher than the cold stream inlet temperature. This type of pinch point generally occurs when one of the fluid streams approaches the critical point (or a phase change) because there are very large changes in the heat capacity of the fluid near the critical point. In the second type of pinch, the heat transfer near the location of the pinch can still be very high because the local heat transfer coefficient experiences a large increase due to the rapidly changing properties caused by the close approach to the critical point.

Because the two recuperators are designed for efficient power generation in a recompression cycle at the maximum expected operating conditions, they are much larger than necessary for the operating conditions used in the recent testing. Therefore, all of the heat that can practically be removed from the hot CO+ fluid stream is transferred to the cold CO$_2$ fluid stream long before the fluid streams exit the two recuperators. This operating condition can be seen in Figure 0-17, where the temperature profile in the HT recuperator is estimated. The calculations used a pressure observed at approximately 5000 s into the power generation test on July 14, 2011, when the loop was operated in the simple recuperated Brayton cycle configuration. The calculation assumed steady-state conditions and fixed increments of heat transfer.

High-Temperature Recuperator State Profiles
DOE SNL Test "GenIV_110714_0952"
At 5000 [s] into the test
Heat Transfer = 688088 [W] ; Heat Loss/Storage = 14342 [W]
Effective UA = 29553 [W/K]
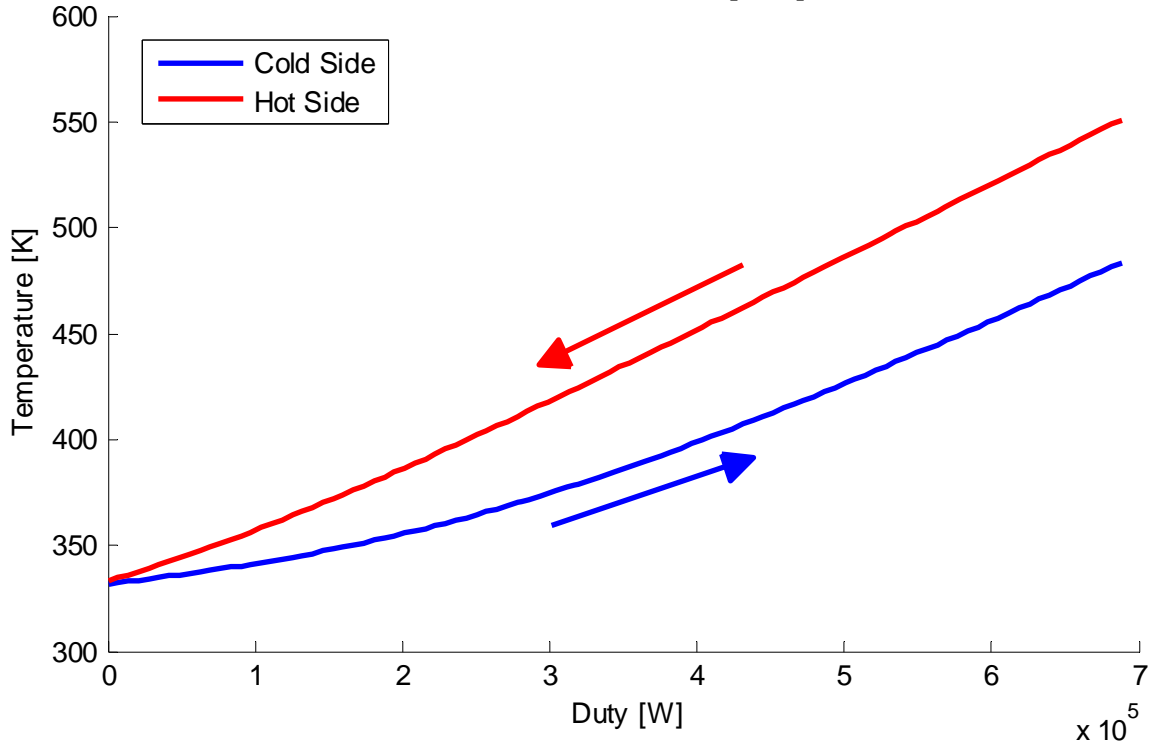
**Figure 0-17. Estimated fluid temperature versus duty within the
HT recuperator at 5000 s into DOE SNL Test "GenIV_110714_0952."**

The temperature profile is plotted as a function of the duty, the amount of heat that has been transferred from the hot fluid into the cold fluid, with a total heat transfer between the streams of 688,088 W. It can be seen that the fluid temperatures approach each other towards the cold-side inlet end of the heat exchanger, resulting in a pinch point temperature difference of about 1°C. Because of this pinch, the effective total conductance-area product (UA) of the HT recuperator, which is related to the effective physical volume of the heat exchanger, is about 30 kW/K, or approximately 50% of the total UA shown in Table 0-1.

Because this pinch point occurs in the HT recuperator, the LT recuperator functions mainly as a thermal mass and a location for heat losses since the hot-side and cold-side inlet temperatures are nearly identical. This behavior can be seen more clearly in Figure 0-18: the heat flow from the cold (low-pressure) side of the LT recuperator to the hot (high-pressure) side of the LT recuperator spikes each time the mass flow rate changes significantly. The heat is stored or removed from the recuperator mass and quickly settles back toward a low level of heat loss and minimal heat transfer as the mass flow stays constant.

Power Balance and Mass Flow Rate
GenIV_110714_0952
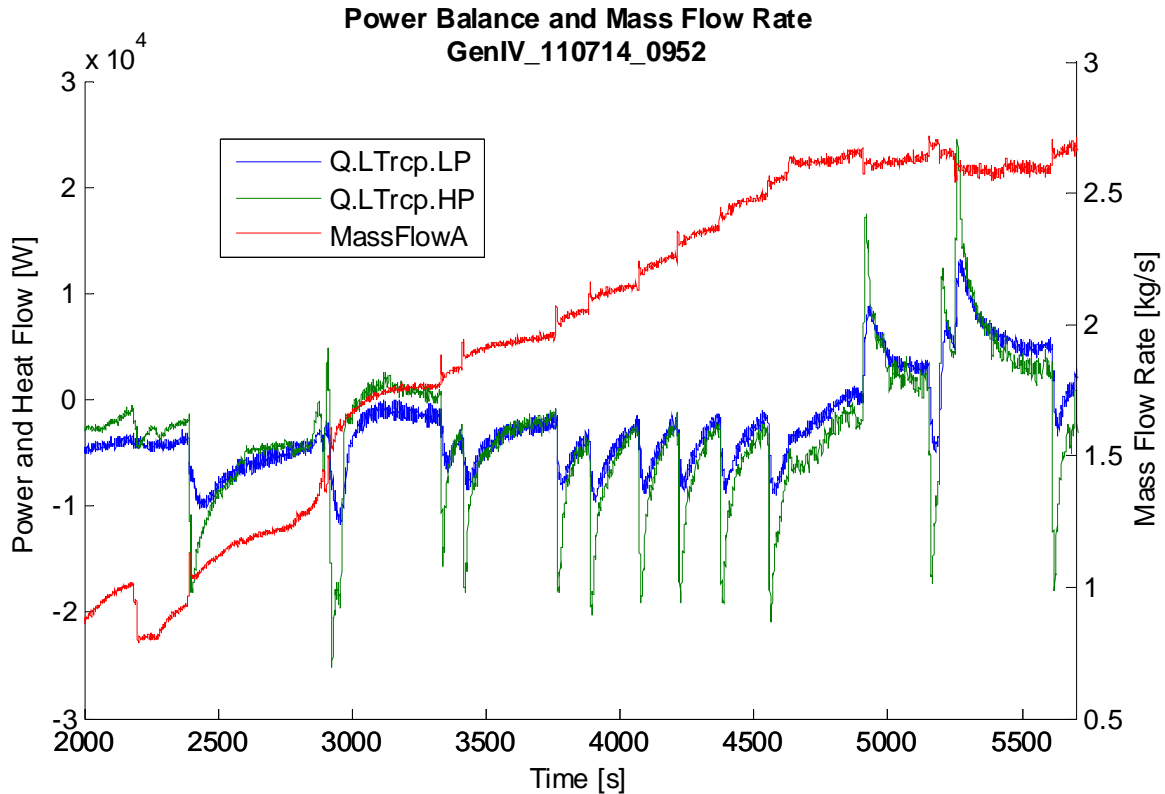
Figure 0-18: The LT recuperator heat flow from the high-pressure side and to the low-pressure side (both positive at design conditions) and the system mass flow rate versus time.

This behavior would be undesirable at design conditions, but since the LT recuperator temperatures are nearly at the ambient temperature, little heat is lost from the system and the main effect of the additional heat exchanger volume at off-design conditions is a slightly slower system response due to the added thermal mass in the recuperators and a slightly larger pressure drop that would not otherwise exist in a system designed for these test conditions.

The T-h diagram for 5000 s into the test, shown in Figure 0-19, clearly indicates that the LT recuperator inlet and outlet states are nearly identical and that they have almost no steady-state impact on the cycle. The HT recuperator, HP inlet, and low-pressure outlet temperatures are also nearly identical, indicating that the maximum amount of heat that can be transferred from the hot CO_2 stream has been transferred to the low CO_2 stream.

T-h Diagram
DOE SNL Test "GenIV_110714_0952"
At 5000 [s] into the test
Generated Power = 11528 [W]

State	1	2	3	4	5	6	7	8
T (K)	306	332	331	483	589	555	333	331
h (kJ/kg)	357	375	374	636	763	731	458	458
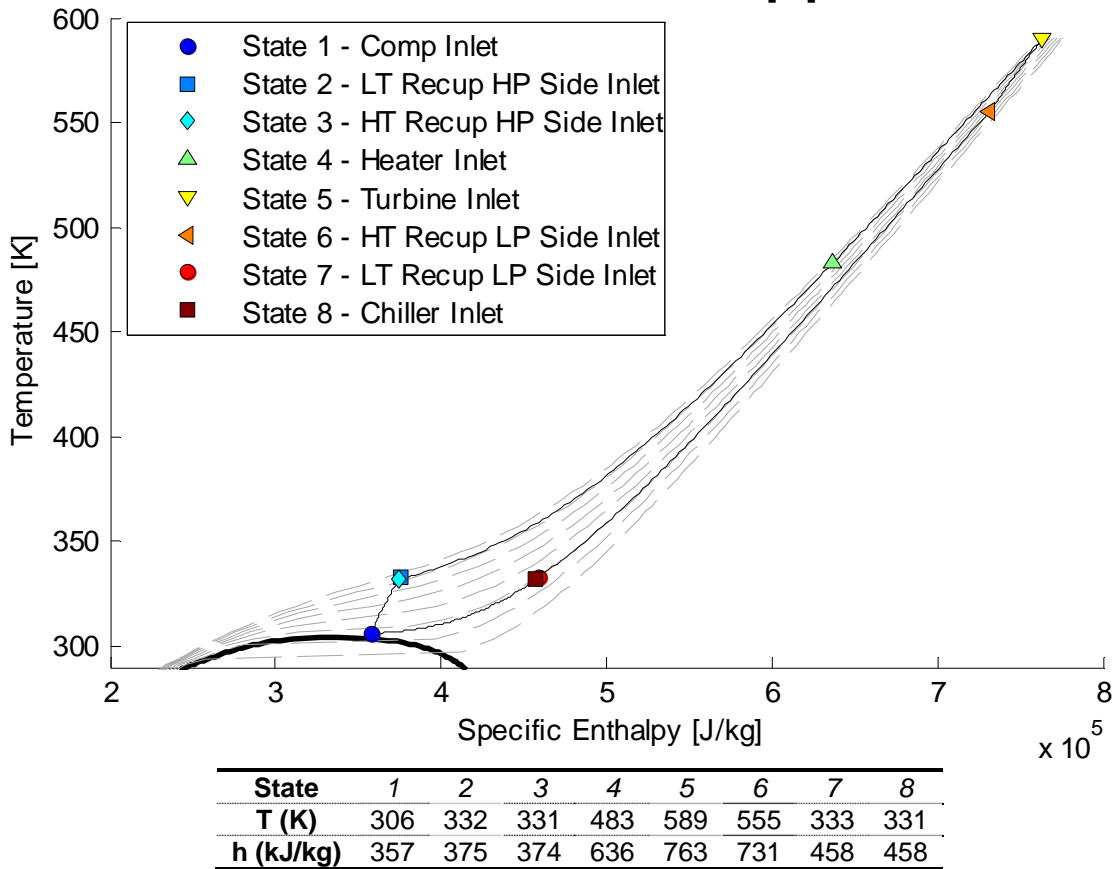
Figure 0-19. A T-h diagram of the system at 5000 s into DOE SNL Test "GenIV_110714_0952."

Note that because the LT recuperator is not transferring significant heat, state points associated with it coincide with others. The mass flow rate through the loop at this time is 2.61 kg/s.

CONCLUSIONS

Overall, research on the S-CO$_2$ Brayton cycle made substantial progress for this milestone as a result of the recent hardware upgrades, which include two new heaters, a new HT recuperator, high-temperature piping, and an improved scavenging pump system. Testing in support of the milestone has continued in the simple recuperated Brayton configuration—using one turbine, one compressor, and one undivided flow path, rather than a split-flow recompression cycle—but this work has progressed to higher temperatures and higher speeds and new record highs in electrical generation.

Tests performed using the main compressor on TAC-A provided insight into the correct operation of the Hydro-Pac pump, and how best to incorporate it into the system as a whole. Using TAC-A, the facility was started up from room temperature conditions using the turbine bypass valve introduced in earlier work, and gradually pushed towards break-even conditions. After numerous runs in the simple Brayton configuration, this process is now relatively routine using either TAC-A and TAC-B. It was also observed that for this power level in the simple Brayton configuration, far too much recuperation capability is installed. Unfortunately, flow from the new scavenging pump interfered with steady compressor inlet conditions, prompting mass flow oscillations that prevented pushing the system further into power production.

When this was repaired, testing began anew using TAC-B, the recompressor turbomachinery. Building upon the experience gained using TAC-A, together with the upgraded cycle hardware, these tests quickly proceeded towards speeds and powers never before attained with this facility (51,000 rpm and 20 kWe). Bearing temperatures remained cool, demonstrating that long periods of operation at steady-state are feasible. Though the recompressor wheel was operated at off-design conditions very near the critical point (main compressor conditions), the loop was able to attain the design flow rates and a pressure ratio of 1.65 at two thirds the design speed. This unexpectedly high performance prompted researchers to consider a design change—enlarging the main compressor diameter. The generation of a significant amount of power for the first time also brought to light inefficiencies in electrical generation that need to be addressed.

Based on these observations, a path forward has been developed for FY2012 testing. This work will center on further pushing power production in the simple Brayton mode, then developing a procedure for bringing the loop from cold-startup to power generation using the full split-flow recompression design capabilities of this facility. Once in the split-flow configuration, the loop will be able to take advantage of both recuperators, boosting power conversion efficiency. To support this effort, more hardware upgrades are needed, including high-temperature upgrades to more piping, the installation of cold-side expansion tanks, and the installation of OSRs for emergency shutdown scenarios. Research will also address methods to reduce inefficiencies in generation. Finally, FY2012 will bring improvement to existing steady-state and dynamic models of the cycle to verify analytical methods, with an eye towards improved predicting of the performance of future multi-megawatt systems through modeling.

REFERENCES

1. Dostal, V., M. Driscoll, and P. Hejzlar, *A Supercritical Carbon Dioxide Cycle for Next Generation Nuclear Reactors,* MIT-ANP-TR-100. Massachusetts Institute of Technology Center for Advanced Nuclear Energy Systems, Cambridge, MA, March 2004.

2. Barber-Nichols Incorporated, http://www.barber-nichols.com, Arvada, CO, U.S., 2011.

3. Heatric Division of Meggitt (UK) Limited, http://www.heatric.com, Dorset, United Kingdom, 2011.

4. Watlow Electric Manufacturing Company, www.watlow.com, St. Louis, Missouri, March 2008.

Distribution

1	MS0771	Andrew Orrell	6200
1	MS0736	Tito Bonano	6220
1	MS1136	Gary Rochau	6221
1	MS1136	Thomas Conboy	6221
1	MS1136	David Ames	6221
1	MS1136	Tom Lewis	6221
1	MS1136	Steve Wright	6221
1	MS1136	Jim Pasch	6221
1	MS1136	Darryn Fleming	6221
1	MS0899	Technical Library	9536